

Learning Network Representations with Disentangled Graph Auto-Encoder

Di Fan

fandi@zju.edu.cn

Chuanhou Gao

gaochou@zju.edu.cn

School of Mathematical Sciences, Zhejiang University, Hangzhou 310058, China

Abstract

The (variational) graph auto-encoder is extensively employed for learning representations of graph-structured data. However, the formation of real-world graphs is a complex and heterogeneous process influenced by latent factors. Existing encoders are fundamentally holistic, neglecting the entanglement of latent factors. This not only makes graph analysis tasks less effective but also makes it harder to understand and explain the representations. Learning disentangled graph representations with (variational) graph auto-encoder poses significant challenges, and remains largely unexplored in the existing literature. In this article, we introduce the Disentangled Graph Auto-Encoder

(DGA) and Disentangled Variational Graph Auto-Encoder (DVGA), approaches that leverage generative models to learn disentangled representations. Specifically, we first design a disentangled graph convolutional network with multi-channel message-passing layers, as the encoder aggregating information related to each disentangled latent factor. Subsequently, a component-wise flow is applied to each channel to enhance the expressive capabilities of disentangled variational graph auto-encoder. Additionally, we design a factor-wise decoder, considering the characteristics of disentangled representations. In order to further enhance the independence among representations, we introduce independence constraints on mapping channels for different latent factors. Empirical experiments on both synthetic and real-world datasets show the superiority of our proposed method compared to several state-of-the-art baselines.

Keywords: Graph auto-encoder, disentangled representation learning

1 Introduction

Graph-structured data has become exceptionally prevalent in the era of big data, spanning across various domains, including social networks, co-authorship networks, biological networks and traffic networks, etc. Represented in the form of graphs, these data illustrate the complex interconnections among entities, reflecting intricate and extensive networks of relationships.

The field of graph analysis includes many significant tasks. Link prediction (Loehlin, 2004; Wang et al., 2008; Daud et al., 2020; Wang et al., 2021; Son et al., 2023) is one of the best-known tasks for predicting missing or possible connections within a graph.

For example, in social networks, link prediction helps with precise targeting in target marketing, which can guide marketing strategies. In biological networks, it is utilized to predict connections between molecules, while in terrorist networks, it assists in identifying suspicious individuals. Other popular graph analysis tasks include node clustering (Wang et al., 2021; Tsitsulin et al., 2023) and node classification (Bhagat et al., 2011; Xiao et al., 2022; Luan et al., 2023). Node clustering aims to group nodes in a graph, where nodes in each cluster are highly relevant. This task finds extensive applications across various domains, including social networks, biology, network security, logistics, finance, and medical image analysis. For instance, in biological networks, it can identify functional modules or groups of genes that work together. Node classification involves assigning predefined labels to nodes based on their attributes, and this task is crucial for understanding the characteristics of individual nodes within a graph. For instance, it can help predict the topics or fields of research papers in citation networks.

However, due to the extensive and highly sparse nature of graphs, graph analysis tasks are often challenging. Therefore, there has been a growing interest in enhancing the learning of graph representations (Perozzi et al., 2014; Hamilton et al., 2017; Wang et al., 2016, 2017; Goyal et al., 2018; Wang et al., 2022). The node representation learning tasks form the foundation of the network analysis tasks mentioned earlier. One particularly successful model for unsupervised node representation learning is the Variational Graph Auto-Encoder (VGAE) and the Graph Auto-Encoder (GAE) (Kipf et al., 2016a). They all consist of an encoder responsible for learning latent representations and a decoder tasked with reconstructing the graph structure data using the learned representations. Their primary goal is to accomplish the task of link prediction. As a result,

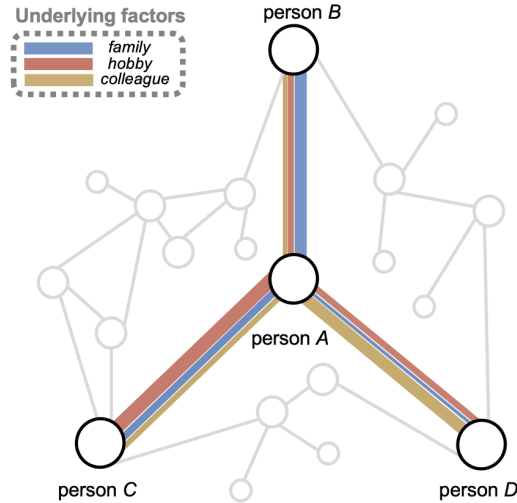


Figure 1: An illustrative social network example that inspired our work. We consider the reasons for interactions between two individuals annotated with lines of different colors, where the thickness of the lines represents the primary determining factor for interaction frequency.

the decoder is relatively straightforward, relying solely on the inner product of the latent representations of the nodes involved for link predictions. However, the encoder is only built upon the original Graph Convolutional Networks (GCN) (Kipf et al., 2016b).

Despite the success of auto-encoder models, existing methods often employ GCN in the encoder, taking a holistic approach and treating the graph as a perceptual whole (Kipf et al., 2016a; Hasanzadeh et al., 2019; Grover et al., 2019; Khan et al., 2021; Shi et al., 2020; Sun et al., 2021; Li et al., 2023). They ignore subtle differences between various relationships in the graph. In fact, graph formation in the real world is a complex, heterogeneous process driven by latent factors. Figure 1 illustrates the concept of disentanglement. It is evident that this social network is inherently heterogeneous, with connections between the four individuals formed for different underlying

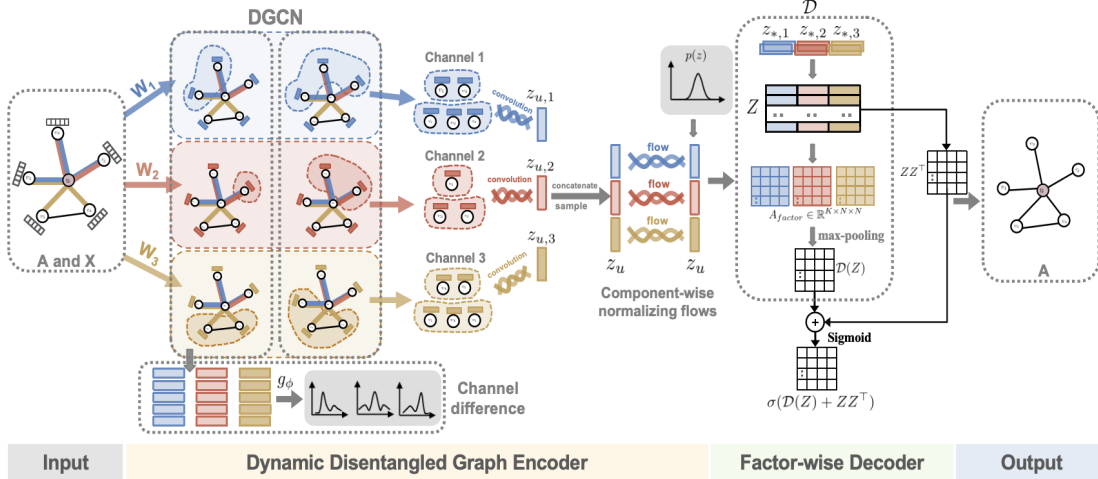


Figure 2: The whole framework of the proposed DVGA. It takes in nodes and their neighbors along with their feature vectors. The dynamic disentangled encoder utilizes DGCN, where the dynamic assignment mechanism considers neighborhoods induced by K different factors and additionally accounts for neighborhoods in the k -th component space. After channel-wise convolution, the resulting component representations are merged and fed into flows for learning disentangled node representations, which are then input into a factor-wise decoder to reconstruct the adjacency matrix. A classifier g_ϕ is employed to promote the independence of disentangled representations across different latent factors. The joint optimization of the factor-wise auto-encoder and independence regularization enhances the disentanglement. In this example, we assume the existence of three latent factors, each corresponding to one of the three channels. factors. Moreover, their interactions exhibit distinct emphases. For instance, the interaction between person A and person B is primarily due to familial ties, while person A and person C engage more due to a shared hobby. Additionally, it's worth noting that connections between every pair of individuals occur due to multiple factors, but the emphasis varies. Without this fine-grained distinction in relationships, representing

nodes only from binary graph structures becomes challenging. This not only hinders the interpretability of learned representations, but also lead to reduced performance of downstream tasks. Therefore, this complexity urges the encoder to disentangle factors, an aspect overlooked by the existing holistic approaches.

In this paper, we propose learning disentangled node representations. While disentangled representation learning, which aims to characterize various underlying factors in factorized representations, has shown many advantages (Higgins et al., 2018), it faces three challenges in graph auto-encoder models. (1) Designing a graph encoder for disentangled representations requires careful planning to guarantee it can effectively infer latent factors with enough expressiveness. (2) Designing a decoder for disentangled representations involves considering factor information in node connections to improve link prediction accuracy. (3) Designing a training scheme to enhance representation independence involves establishing statistical independence between different parts of representations corresponding to different latent factors, thereby improving the quality of disentangled representations.

To tackle the aforementioned challenges, we introduce innovative auto-encoder models for learning disentangled graph representations, that is, Disentangled Variational Graph Auto-Encoder (DVGA) and Disentangled Auto-Encoder (DGA). Initially, we design a Disentangled Graph Convolutional Network (DGCN) using dynamic assigning mechanism (Zheng et al., 2021), incorporating multiple channels to aggregate information related to each disentangled latent factor. It facilitates the learning of disentangled latent representations. Subsequently, a component-wise flow is applied to each channel to enhance the expressiveness of individual representations, promoting the disentangled

representations to best capture representations related to latent factors in the graph. Furthermore, we design a factor-wise decoder, ensuring that if there is any factor leading to a connection between nodes, then these two nodes are connected in the final prediction result. This decoder improves the performance of downstream tasks. Additionally, to encourage the independence of representations corresponding to different latent factors, we introduce independence constraints to the mapping channels of different latent factors. Finally, the auto-encoder and independent regularization will be co-optimized within a unified framework, empowering the disentangled graph encoder to generate superior disentangled graph representations while enhancing overall model performance. In comparison to existing methods, our models learn disentangled representations from the graph, allowing for exploration of the meaning of each channel, thereby improving interpretability and generating convincing and understandable link prediction results.

Our contributions can be summarized as follows:

- We introduce two novel disentangled graph auto-encoder models: the Disentangled Variational Graph Auto-Encoder (DVGA) and the Disentangled Graph Auto-Encoder (DGA). The DVGA model incorporates a disentangled encoder, component-wise flow, factor-wise decoder, and an independence regularization term in the loss function to learn disentangled representations. Simultaneously, the DGA model is similarly presented. To the best of our knowledge, we are among the very few researchers investigating disentangled graph auto-encoder models.
- Our proposed disentangled graph convolutional network in the encoder captures multiple factors by learning disentangled latent factors on graphs, enabling multi-

relation disentangling. We enhance the expressive capability of each channel representation through flow, further boosting the overall capabilities of the representation. The designed decoder is tailored for disentangled representations, improving its ability to predict graph structures.

- To validate the effectiveness of our proposed models, we conduct comprehensive experiments on both synthetic datasets and real-world datasets. The results on several datasets demonstrate that DVGA and DGA achieves state-of-the-art performance, significantly outperforming the baselines both quantitatively and qualitatively.

The subsequent sections of the paper are structured as follows. In section 2, we discuss the methods of graph embedding and review the closely related work on disentangled representation learning in the context of the graph auto-encoder. Section 3 provides an introduction to the preliminaries and the problem formulation. In section 4, we propose our models, including DVGA and DGA, along with their optimization objectives and algorithms. In section 5, we derive the algorithm’s time complexity and analyze the number of algorithm’s parameter. In section 6, we present quantitative and qualitative experiments as well as model ablation, convergence behavior, and complexity analysis. The conclusion in the final section emphasizes the innovation of our approach and suggests potential directions for future research.

2 Related Work

2.1 Graph Embedding

The goal of graph embedding is to embed graph-structured data into a low-dimensional feature space while preserving the graph information. We classify graph embedding algorithms into two main types: topological embedding methods and content-enhanced embedding methods (Cai et al., 2018; Pan et al., 2018).

Topological embedding methods only utilize the topological structure of the graph, aiming to maximally preserve the topological information. The DeepWalk model, introduced by Perozzi et al. (2014), learned node embeddings by random walks. Later, various probabilistic models have been proposed, such as LINE (Tang et al., 2015) and node2vec (Grover et al., 2016). Matrix factorization methods like HOPE (Ou et al., 2016) and M-NMF (Wang et al., 2017) have been developed to learn the latent representation of the graph, which leveraged the adjacency matrix. In the work by Xingyi et al. (2021), node representations were generated by learning proximity measures and singular value decomposition decomposition parameters within a comprehensive framework. Deep learning models (Zaiqiao et al., 2019) have also been employed for graph embedding, such as SDNE (Wang et al., 2016) and DNGR (Cao et al., 2016).

Content-enhanced embedding methods leverage both topological information and content features. Yang et al. (2015) introduced TADW which extends its matrix factorization model to support embedding of attribute information. UPP-SNE (Zhang et al., 2017) employed an approximate kernel mapping method to improve the learning of user embeddings in social networks using user profile features. Deep learning models

such as GCN (Kipf et al., 2016b), GraphSAGE (Hamilton et al., 2017), GAT (Velickovic et al., 2017; Brody et al., 2021) and GSN (Bouritsas et al., 2022) can also learn node representations through supervised tasks. Some works (Kipf et al., 2016a; Simonovsky et al., 2018) were based on generative models, specifically using Variational Auto-Encoder (VAE) (Kingma et al., 2013) on graphs for learning representations. A comprehensive discussion on this topic will be provided in the subsequent subsection.

2.2 Extended (Variational) Graph Auto-Encoder

With the rapid development of deep learning, there has been an increasing focus on research in graph representation learning using generative models. Inspired by AE and VAE (Kingma et al., 2013), Variational Graph Auto-Encoder (VGAE) and the Graph Auto-Encoder (GAE) (Kipf et al., 2016a) utilized GCN as encoders and inner products as decoders. They accomplished link prediction tasks while learning embeddings for each node in the graph.

In recent years, significant progress has been made in enhancing the structure of these models. LGAE (Salha et al., 2021) employed significantly simpler and more interpretable linear models as encoder, achieving comparable performance across various real-world datasets. NF-VGA (Shan et al., 2020) designed a prior-generative module to generate a flexible distribution as the prior for latent representations. SIG-VAE (Hasanzadeh et al., 2019) enhanced the generative modeling by employing a hierarchical variational framework.

In terms of decoders, TVGA (Shi et al., 2020) leveraged the triadic closure property to introduce a triad decoder. The triad decoder collectively predicts the three edges

within a local triad to improve link prediction tasks. Graphite (Grover et al., 2019) employed an innovative iterative refinement strategy for graphs, inspired by low-rank approximations. In terms of model training improvements, ARGAs and ARVGAs (Pan et al., 2018) introduced a novel adversarial graph embedding method.

Recently, there have also been additional improvements from the point of refining priors and other aspects of the model (Ahn et al., 2021; Davidson et al., 2018; Sun et al., 2021; Khan et al., 2021). However, current approaches based on VGAE or GAE have only explored general settings in handling entanglement situations. Their encoders, lacking the integration of disentangled representation learning, are challenged by recognizing and disentangling the heterogeneous latent factors hidden in the observed graph-structured data. Thus, these holistic encoding approaches exhibit limited capabilities in learning graph representations and often lead to less satisfactory performance in link prediction tasks and other downstream applications.

2.3 Disentangled representation learning

Learning disentangled representation is to obtain a factorized representation which can effectively identify and disentangle the underlying explanatory factors in observed data (Bengio et al., 2013). Due to its capability to generate robust and interpretable representations, disentangled representation learning has become a central challenge in the field of machine learning.

The majority of existing research can be found in the field of computer vision, where variational methods based on VAE are widely employed for disentangled representation learning in images (Burgess et al., 2018; Higgins et al., 2016; Chen et al., 2018; Trauble

et al., 2021; Kim et al., 2018; Locatello et al., 2020; Kim et al., 2019; Shen et al., 2022).

This is primarily achieved by imposing independent constraints on the posterior of the latent variable through KL divergence.

The exploration of disentangled representation learning for graph-structured data has recently captured significant attention. In many cases, the relationships between nodes in a homogeneous graph remain heterogeneous, entangled, but they are solely represented as single binary-valued edges. However, edges in the graph often carry extensive relationship information beyond binary indicators of structural connectivity. So this motivation prompts us to implicitly discover the underlying relationships between entities. DisenGCN (Ma et al., 2019) stood out as an innovative contribution in graph disentanglement. It focuses on the generation of independent latent features to achieve disentanglement at the node level. However, it did not take into account multiple potential relationships between entities. Later, ADGCN (Zheng et al., 2021) considered the existence of multiple relationships between nodes and utilized an adversarial regularizer to enhance separability among different latent factors. Related works mainly concentrate on node-level (Guo et al., 2022; Liu et al., 2020), edge-level (Zhao et al., 2022; Wu et al., 2021), and graph-level (Wu et al., 2022; Yang et al., 2015) disentanglement representation learning. Furthermore, another line of work employs a self-supervised learning strategy to obtain disentangled representations (Xiao et al., 2022; Li et al., 2021; Zhang et al., 2023). This includes the design of heuristic proxy tasks and integration with contrastive learning. Simultaneously, there has been a considerable amount of research on disentangled representation learning for heterogeneous graph (Wu et al., 2021; Wang et al., 2020; Geng et al., 2022). Nevertheless, these works either typically

rely on supervised labels and primarily focus on node classification tasks, or they concentrate on other specific application domains. In contrast, our emphasis is on utilizing generative models to learn disentangled node embedding for graph-structured data, and focusing on link prediction and other downstream tasks.

Currently, the exploration of disentangled representation learning for graphs through generative models, i.e. (variational) graph auto-encoder, is largely unexplored. There is only one nearly contemporaneous work that addresses this, but only focusing on link prediction task (Fu et al., 2023). In their proposed model, they incorporate an neighborhood routing mechanism (Ma et al., 2019) to achieve disentangled node embeddings. However, a drawback is that it assumes relationships between nodes are only influenced by one single factor. On the contrary, our models not only employ a more general mechanism to learn representations but also enhances the inference model’s capability through flow models. Additionally, we use a factor-wise decoder that better aligns with the link prediction task emphasized in generative models. Our objective is to learn disentangled node representations. This not only improves performance in link prediction tasks but also demonstrates outstanding results in other downstream tasks.

3 Preliminaries and Problem Formulation

In order to better describe the issues that our article focuses on and introduce our work, we first briefly review the idea of GAE and VGAE in section 3.1 and then formulate the problems we are concerned about in section 3.2.

3.1 Preliminaries on (Variational) Graph Auto-Encoder

VGAE and GAE introduced by Kipf et al. (2016a) are frameworks designed for unsupervised learning on graph-structured data. One notable feature is their natural ability to incorporate node features, leading to a substantial improvement in predictive performance on different tasks across various benchmark datasets.

We will primarily focus on undirected graphs, though the approach can be easily extended to directed graphs. Let us begin by introducing some notations. Consider a graph $G = (V, E, X)$, where V is the set of N nodes, and E is the set of edges. For any distinct nodes i and j , if there's an edge connecting them, we denote it as $(i, j) \in E$. The topological structure of the input graph G can be expressed using an adjacency matrix $A \in \mathbb{R}^{N \times N}$ where $A_{i,j} = 1$ if $(i, j) \in E$, and $A_{i,j} = 0$ otherwise. Its degree matrix is D . $X \in \mathbb{R}^{N \times f}$ is the node feature matrix, where each node $i \in V$ has a feature vector $x_i \in \mathbb{R}^f$, and f is the dimension of raw features per node. The matrix for graph embeddings is $Z \in \mathbb{R}^{N \times d}$, with $z_i \in \mathbb{R}^d$ representing the embedding of node i .

GCN is used as the encoder in Kipf et al. (2016a), which is designed specifically for processing and extracting information from graph-structured data. For a L -layer GCN, its message propagation rule is defined by the following formula:

$$H^{(l+1)} = f_{\theta}(H^{(l)}, A) = \text{Relu}(\tilde{D}^{\frac{1}{2}} \tilde{A} \tilde{D}^{-\frac{1}{2}} H^{(l)} W^{(l)}). \quad (1)$$

Here, θ is the parameters of the encoder, $\tilde{A} = A + I_N$, I_N is the identity matrix, $\tilde{D}_{ii} = \sum_{j=1}^N \tilde{A}_{ij}$ and $W^{(l)}$ is the parameters of weight matrix. $\text{Relu}(\cdot)$ denotes the Relu activation function. $H^{(l)}$ is the matrix of activations in the l -th layer, $H^{(0)} = X$

and $H^{(L)} = Z$. In GAE, Kipf et al. (2016a) used two-layer GCN as the encoder:

$$H^{(1)} = f_{\theta}(X, A), Z = f_{\theta}(H^{(1)}, A). \quad (2)$$

In VGAE, the posterior distribution of the embedding vectors is given by the following formulation:

$$q_{\theta}(Z|X, A) = \prod_{i=1}^N q_{\theta}(z_i|X, A), \quad (3)$$

$$\text{with } q_{\theta}(z_i|X, A) = \mathcal{N}(\mu_i, \text{diag}(\sigma_i^2)), \quad (4)$$

where μ_i and $\log \sigma_i^2$ are learned from two GCNs with shared first-layer training parameters. Samples of $q(Z|X, A)$ can be obtained by using the reparameterization trick (Doersch, 2016).

The decoder is based on the inner product between latent representations of each pair of nodes. In the case of GAE, the reconstruction of the adjacency matrix A is formulated as follows:

$$A = \sigma(ZZ^T). \quad (5)$$

where σ is typically the sigmoid function. For VGAE, the decoder is probabilistic and is defined by the inner product between latent variables. This can be expressed as follows:

$$p(A|Z) = \prod_{i=1}^N \prod_{j=1}^N p(A_{ij}|z_i, z_j), \quad (6)$$

$$\text{with } p(A_{ij}|z_i, z_j) = \sigma(z_i^T z_j). \quad (7)$$

The training objective for VGAE is to recover information about the graph from the graph embedding matrix Z . Therefore, our aim is to learn the model parameters by

maximizing the log marginal distribution which can be lower-bounded by ELBO:

$$\log p_\theta(A|X) = \log \int q_\theta(Z|X, A) \frac{p(Z)p(A|Z)}{q_\theta(Z|X, A)} dZ \quad (8)$$

$$\geq \int q_\theta(Z|X, A) \log \frac{p(Z)p(A|Z)}{q_\theta(Z|X, A)} dZ \quad (9)$$

$$= \mathbb{E}_{Z \sim q_\theta(Z|X, A)} \log p(A|Z) + \mathbb{E}_{Z \sim q_\theta(Z|X, A)} \log \frac{p(Z)}{q_\theta(Z|X, A)} \quad (10)$$

$$= \mathbb{E}_{Z \sim q_\theta(Z|X, A)} \log p(A|Z) - D_{KL}(q_\theta(Z|X, A) || p(Z)). \quad (11)$$

Here, the inequality is derived from Jensen’s inequality (Weisstein, 2006), and $D_{KL}(\cdot || \cdot)$ represents the Kullback-Leibler (KL) divergence (Kullback et al., 1951). We set $p(Z)$ to be a Gaussian normal distribution, i.e.,

$$p(Z) = \prod_{i=1}^N p(z_i) = \prod_{i=1}^N \mathcal{N}(z_i | 0, I). \quad (12)$$

For GAE, the non-probabilistic variant of VGAE, the training objective involves a simple reconstruction loss:

$$\mathcal{L}_{recon} = -\mathbb{E}_{Z \sim q_\theta(Z|X, A)} \log p(A|Z). \quad (13)$$

3.2 Problem Formulation

For (variational) graph auto-encoder, the objective is to learn a graph encoder $f_\theta(\cdot)$ with parameters θ that outputs interpretable low-dimensional stochastic latent variables $Z = f_\theta(G) \in \mathbb{R}^{N \times d}$ ($d \ll n$). Simultaneously, such learned node representations, similar to other node representation learning methods, are capable of tackling a diverse range of tasks related to nodes. Here, our primary focus is on the classical task of link prediction for nodes, aligning with the experiments conducted in Kipf et al. (2016a).

In our study, we aim to improve the link prediction performance in (variational) graph auto-encoder by improving its overall framework, with the primary goal of learn-

ing disentangled node representations through the disentangled graph encoder f_θ . For each node u , the output z_u from the disentangled encoder will be a disentangled representation. Specifically, assuming there are K latent factors to be disentangled, z_u is composed of K independent components, i.e., $z_u = [z_{u,1}, z_{u,2}, \dots, z_{u,K}]$, where $z_{i,k} \in \mathbb{R}^{\frac{d}{K}}$ ($1 \leq k \leq K$). The k -th component $z_{u,k}$ is used to characterize aspects of node u that are related to the k -th latent factor.

Here, we assume the underlying factors generating observed graph-structured data are mutually independent, which is a common premise in the field of disentangled representation learning (Higgins et al., 2018; Bengio et al., 2013). Our goal is to learn factorized and expressive representations where each component is independent and exclusively corresponds to a single ground-truth factor behind the graph formulation. This is intended to enhance the completeness of each node’s representation, resulting in more effective node descriptions and improved performance in graph analytic tasks.

4 Proposed Mechanism

This section presents the DVGA model, with its framework illustrated by Figure 2. In the end, we also introduce its non-probabilistic variant, the DGA model.

4.1 Dynamic Disentangled Graph Encoder

Here, our goal is to introduce the disentangled graph encoder that can learn disentangled node embeddings. Essentially, it comprises the disentangled graph convolutional neural network, which we refer to as DGCN. We assume that each node consists of K indepen-

dent components, indicating the presence of K latent factors that need to be disentangled. For a node $u \in V$, its hidden representation z_u is expressed as $[z_{u,1}, z_{u,2}, \dots, z_{u,K}]$, where $z_{u,k} \in \mathbb{R}^{\frac{d}{K}}$ ($1 \leq k \leq K$) is used to describe k -th aspects of node u .

Firstly, we project the feature vector x into K different subspaces to initialize the embedding vectors for K channels:

$$c_{u,k} = \frac{W_k^\top x_u + b_k}{\|W_k^\top x_u + b_k\|_2}, \quad (14)$$

where $W_k \in \mathbb{R}^{n \times \frac{d}{K}}$ and $b_k \in \mathbb{R}^{\frac{d}{K}}$ are the parameters of k -th subspace. For a comprehensive understanding of aspect k for node u , we need to extract information from the neighborhood of u . This involves constructing $z_{u,k}$ using both $c_{u,k}$ and $\{c_{v,k} : (u, v) \in E\}$. Next, we provide three hypotheses for the relationships between nodes:

Hypothesis 1: The generation of links between nodes result from the interaction of various hidden factors.

Hypothesis 2: If there is similarity in the k -th component space between node u and its neighboring node v , it indicates that the link between the two nodes may be attributed to factor k .

Hypothesis 3: If neighbors exhibit similarity in aspect k , forming a cluster in the k -th subspace, it is plausible that factor k is responsible for connecting node u with this specific group of neighbors.

Hypothesis 1 aligns with our realistic understanding of the reasons behind the formation of graphs. It suggests that the links between nodes can be influenced by various factors. In comparison to previous research on disentanglement, this hypothesis is closer to real-world situations (Liu et al., 2020; Ma et al., 2019). For example, in a friendship network, the acquaintance between two individuals may result from re-

relationships such as colleagues, classmates, or shared interests. **Hypotheses 2 and 3** correspond to the first-order and second-order proximities within the topological structure influenced by factor k , respectively (Tang et al., 2015). This insight also inspires us to explore K subspaces to identify latent factors.

Building upon these three hypotheses, we learn the disentangled representations of nodes by leveraging dynamic assignment mechanism (Zheng et al., 2021), which is a disentangle layer:

$$z_{u,k}^t = c_{u,k} + \alpha \sum_{v:(u,v) \in E} p_{u,v}^{k,t-1} c_{v,k} + \beta \sum_{v:(u,v) \in E} q_{v,u}^{k,t-1} c_{v,k} \quad (15)$$

$$p_{u,v}^{k,t} = \frac{\exp(c_{v,k}^\top z_{u,k}^t)}{\sum_{k=1}^K \exp(c_{v,k}^\top z_{u,k}^t)} \quad (16)$$

$$q_{v,u}^{k,t} = \frac{\exp(c_{v,k}^\top z_{u,k}^t)}{\sum_{v:(u,v) \in E} \exp(c_{v,k}^\top z_{u,k}^t)} \quad (17)$$

$$z_{u,k}^t = \frac{z_{u,k}^t}{\|z_{u,k}^t\|_2} \quad (18)$$

where iteration $t = 1, 2, \dots, T$. $p_{u,v}^k$ represents the probability of the connection between nodes v and u attributed to the k -th factor, while $q_{v,u}^k$ denotes the importance of aggregating node v with respect to node u in the k -th component space. They satisfies $p_{u,v}^k \geq 0$, $q_{v,u}^k \geq 0$, $\sum_{k=1}^K p_{u,v}^k = 1$ and $\sum_{k=1}^K q_{v,u}^k = 1$. α and β serve as trade-off coefficients and we treat them as trainable parameters and adjust their range to be within $(0, 1)$. The dynamic assignment mechanism will iteratively infer $p_{u,v}^k, q_{v,u}^k$ and construct $z_{u,k}$. Meanwhile, this mechanism enables the coexistence of multiple relationships between nodes. It's important to note that there are a total of L disentangle layers, and in each layer $l \leq L - 1$, the value of $c_{u,k}$ is ultimately assigned as $z_{u,k}^T$. For additional details, please refer to Algorithm 1.

The final disentangled embedding of node u output by DGCN is the concatenation

of components learned across all K channels, i.e.,

$$z_u = \text{concatenate}(z_{u,1}, z_{u,2}, \dots, z_{u,K}). \quad (19)$$

Subsequently, by applying Eqs. (2), (3), (4) and replacing GCN with DGCN, we obtain the dynamic disentangled graph encoder.

In contrast to existing holistic graph encoders, the dynamic disentangled graph encoder comprises K channels, enabling the identification of complex heterogeneous latent factors and the depiction of multiple relation aspects.

4.2 Enhancing Posterior Flexibility through Component-wise Normalizing Flows

We observe that when the inference process relies solely on the dynamic disentangled graph encoder, DVGA will typically output a factorized distribution. This implies that the individual component representation $z_{u,k}$ are not only independent of each other but also mutually independent for each d -dimensional vectors. The latter is neither necessary nor desired because we want each d -dimensional component to better capture enough information about each factor. Therefore, in this section, we aim to enhance the flexibility of each d -dimensional component representation.

Normalizing Flows (NF) (Papamakarios et al., 2017) are frequently used to enrich the families of posterior distribution. They impose explicit density functions for the mixing distributions in the hierarchy. Thus, it is sometimes employed in VGAE (Hasanzadeh et al., 2019; Shan et al., 2020) for the purpose of enhancing model flexibility. To better learn the information of each factor, we introduce a flow-based, component-wise

distribution as the posterior distribution for the latent variables in DVGA. This distribution is designed to make the d -dimensional component latent variables, namely, embeddings derived from each channel, better at describing the complex factor properties.

Our main flow process involves applying separate flows to the K components of z_u , with each flow consisting of M steps (e.g., $M = 4$). Each step incorporates an affine coupling layer, which primarily ensures that the latent variable $z_{u,k}$ follows a flexible distribution. Specifically, for each component $1 \leq k \leq K$, we iterate as follows to apply component-wise flows, i.e., for $m = 1, 2, \dots, M$:

$$z_{u,k,1:d'}^{(m)} = z_{u,k,1:d'}^{(m-1)}, \quad (20)$$

$$z_{u,k,d'+1:d}^{(m)} = z_{u,k,d'+1:d}^{(m-1)} \odot \exp(s_k(z_{u,k,1:d'}^{(m-1)})) + t_k(z_{u,k,1:d'}^{(m-1)}). \quad (21)$$

Here, $s_k(\cdot)$ and $t_k(\cdot)$ denote transformation functions (mapping the input from d' to $d - d'$ dimension space), $s(z_{u,k,1:d'}^{(m-1)}) = [s_1(z_{u,k,1:d'}^{(m-1)}), s_2(z_{u,k,1:d'}^{(m-1)}), \dots, s_{d-d'}(z_{u,k,1:d'}^{(m-1)})]^\top$, $t(z_{u,k,1:d'}^{(m-1)}) = [t_1(z_{u,k,1:d'}^{(m-1)}), t_2(z_{u,k,1:d'}^{(m-1)}), \dots, t_{d-d'}(z_{u,k,1:d'}^{(m-1)})]^\top$. The \odot represents the Hadamard product. The output of the affine coupling layer is obtained by concatenating $z_{u,k,1:d'}^{(m)}$ and $z_{u,k,d'+1:d}^{(m)}$. We swap or randomly shuffle the dimensions to enhance the mixing of information between two affine coupling layers.

This process transforms the posterior distribution $q(z|X, A)$ into a more complex distribution, allowing each $z_{u,k}$ to have sufficient expressive capacity while preserving the separability of information between each channel.

4.3 Factor-wise Decoder

Unlike the conventional decoder design in the (Variational) Graph Auto-Encoder and other approaches that broadly utilize graph information to design decoders (Hasanzadeh et al., 2019; Grover et al., 2019; Shi et al., 2020), both DGA and DVGA introduce a novel factor-wise decoder for predicting edge connections between nodes. This design encourages the decoder to integrate information at the factor level, promoting link prediction performance.

As we already know, the formation of real-world graphs is typically influenced by multiple latent heterogeneous factors. Thus, if any factor leads to the existence of a relationship between two nodes, an edge will connect them in the final result. Based on this observation, we modify the traditional decoder. The structure of the proposed decoder is also shown in Figure 2. Firstly, we perform cosine similarity calculation for each K components between each pair of nodes $z_u = [z_{u,1}, \dots, z_{u,K}]^\top$ and $z_v = [z_{v,1}, \dots, z_{v,K}]^\top$. The output vector A_{factor} is in $\mathbb{R}^{K \times N \times N}$, corresponding to predicting the connection status of nodes in K component spaces associated with K factors. The result of each component space connection corresponds to an $N \times N$ matrix. This vector A_{factor} is then fused by performing a max-pooling operation on the prediction of each two-node connection of the K channels to obtain the final edge connection state. The entire block, denoted as \mathcal{D} , is ultimately merged with inner products constructed from Z . This extra inner product connection functions in a manner similar to the residual connections found in residual networks (He et al., 2016). Finally, the output of the factor-wise decoder is as follows:

$$p(A|Z) = \sigma(\mathcal{D}(Z) + ZZ^\top). \quad (22)$$

This decoder function is an expansion of the inner product decoder, as it turns into the conventional inner product decoder when \mathcal{D} outputs a zero mapping.

4.4 Evidence Lower Bound (ELBO)

Now we describe the objective of DVGA, following the paradigm of the VGAE (Kipf et al., 2016a). The model parameters, denoted as θ , are acquired by maximizing the lower bound of log-likelihood, as specified in Eq.(11):

$$\theta^* = \operatorname{argmax}_{\theta} \mathcal{L}_{ELBO}(\theta) \quad (23)$$

$$= \operatorname{argmax}_{\theta} [\mathbb{E}_{Z \sim q_{\theta}(Z|X,A)} \log p(A|Z) - D_{KL}(q_{\theta}(Z|X,A)||p(Z))] \quad (24)$$

The first term corresponds to the reconstruction loss for link prediction, as defined by Eq. (6) and Eq. (22). The second term represents the KL divergence, where the prior $p(Z)$ is formulated by Eq. (12).

Claim. The $q_{\theta}(Z|X, A)$ in Eq. (3) can be computed as follows:

$$\log q_{\theta}(z_u|X, A) = \log q_{\theta}(z_u^{(0)}|X, A) - \sum_{m=1}^M \sum_{k=1}^K \log \left| \frac{df_k^{(m)}}{dz_{u,k}^{(m-1)}} \right| \quad (25)$$

$$= \log q_{\theta}(z_u^{(0)}|X, A) - \sum_{m=1}^M \sum_{k=1}^K \sum_{i=d'+1}^d s_i(z_{u,k,1:d'}^{(m-1)}) \quad (26)$$

where $u \in V$, $z_u = z_u^{(M)}$ and $z_u^{(0)}$ is the latent variable output from the dynamic graph encoder. $f_k^{(m)}$ represents the complete function of the flow for channel k from step $m-1$ to m as described in Eqs. (20) and (21).

Proof. Eqs. (20) and (21) provide the functions of the flow from step $m-1$ to m for the component $z_{u,k}$, denoted as $f_k^{(m)}$. Set $f^{(m)} = [f_1^{(m)}, f_2^{(m)}, \dots, f_K^{(m)}]$. Considering

the following equation,:

$$\begin{aligned}
z_u^{(m)} &= [z_{u,1}^{(m)}, z_{u,2}^{(m)}, \dots, z_{u,K}^{(m)}] \\
&= [f_1^{(m)}(z_{u,1}^{(m-1)}), f_2^{(m)}(z_{u,2}^{(m-1)}), \dots, f_K^{(m)}(z_{u,K}^{(m-1)})] \\
&= f^{(m)}(z_u^{(m-1)}),
\end{aligned} \tag{27}$$

then, we can compute the following Jacobian matrix:

$$\begin{aligned}
\det(J_{f^{(m)}}(z_{u,1}^{(m-1)}, z_{u,2}^{(m-1)}, \dots, z_{u,K}^{(m-1)})) &= \begin{vmatrix} \frac{df_1^{(m)}}{dz_{u,1}^{(m-1)}} & & & \\ & \frac{df_2^{(m)}}{dz_{u,2}^{(m-1)}} & & \\ & & \ddots & \\ & & & \frac{df_K^{(m)}}{dz_{u,K}^{(m-1)}} \end{vmatrix} \\
&= \prod_{k=1}^K \frac{df_k^{(m)}}{dz_{u,k}^{(m-1)}}
\end{aligned} \tag{28}$$

Note that in Eq. (29), we can further use the fact that $\frac{df_k^{(m)}}{dz_{u,k}^{(m-1)}}$ is a lower triangular matrix, yielding:

$$\frac{df_k^{(m)}}{dz_{u,k}^{(m-1)}} = \prod_{i=d'+1}^d \exp(s_i(z_{u,k,1:d'}^{(m-1)})) \tag{30}$$

Finally, we can compute the ultimate formulation as follows:

$$\log q_\theta(z_u|X, A) = \log(q_\theta(z_u^{(0)}|X, A) \left| \det \frac{\partial z_u^{(0)}}{\partial z_u} \right|) \tag{31}$$

$$= \log q_\theta(z_u^{(0)}|X, A) - \log \left| \det \frac{\partial z_u}{\partial z_u^{(0)}} \right| \tag{32}$$

$$= \log q_\theta(z_u^{(0)}|X, A) - \sum_{m=1}^M \log \det \left| \frac{\partial z_u^{(m)}}{\partial z_u^{(m-1)}} \right| \tag{33}$$

$$= \log q_\theta(z_u^{(0)}|X, A) - \sum_{m=1}^M \sum_{k=1}^K \log \left| \frac{df_k^{(m)}}{dz_{u,k}^{(m-1)}} \right| \tag{34}$$

$$= \log q_\theta(z_u^{(0)}|X, A) - \sum_{m=1}^M \sum_{k=1}^K \sum_{i=d'+1}^d s_i(z_{u,k,1:d'}^{(m-1)}). \tag{35}$$

Thus, the proof is complete. \square

In the above proof, the simplicity of the computations are attributed to the affine coupling flow used in Eqs. (20) and (21). In the end, after computing $\log q_\theta(z_u|X, A)$, we can use Eq. (3) and employ the reparameterization trick (Doersch , 2016) to get $D_{KL}(q_\theta(Z|X, A)||p(Z))$, so Eq. (24) can be calculated.

4.5 Statistical Independence of Mapping Subspaces

Strengthening the independence of the disentangled node representations explicitly contributes to the graph encoder’s ability to capture distinct information across various latent factors, potentially enhancing performance in downstream tasks. Next, we provide detailed explanations of independence regularization.

Remind our main goal is to empower the graph encoder to generate disentangled representations $z_u = [z_{u,1}, z_{u,2}, \dots, z_{u,K}]$ for each latent factor. The K different factors extracted by the dynamic routing mechanism are intended to focus on different connecting reasons, with each of the K channels capturing mutually exclusive information related to latent factors. This emphasizes the importance of further promoting statistical independence among the disentangled representations to enhance the disentanglement. Therefore, before performing dynamic assignment mechanism, it is crucial to ensure that the focused perspectives of the K subspaces in Eq. (14) are distinct. Hence, we consider imposing independent constraints on these K subspaces.

Unfortunately, it is not trivial to obtain the solution that all disentangled subspaces are maximally different from each other. Therefore, we consider imposing independence constraints on the initial embedding vectors obtained from projections in K different subspaces, as expressed in Eq. (14). Therefore, we approximate the solution

by assigning unique labels to embedding vectors from the same subspace and optimizing the mapping subspaces as a vector classification problem. The discriminator, as represented in Eq. (36), is to distinguish which label a given embedding vector has:

$$D_k = \text{Softmax}(g_\phi(c_{u,k})), k = 1, 2, \dots, K, \forall u \in V. \quad (36)$$

This discriminator, denoted as g_ϕ , comprises a fully connected neural network, and its parameters is ϕ . It takes the embedding vector $c_{u,k}$ as inputs and generates a subspace-specific label D_k .

We design the following loss to train the discriminator:

$$\mathcal{L}_{reg}(\phi) = -\frac{1}{N} \sum_{i=1}^N \left(\sum_{e=1}^{N_k} \mathbb{1}_{k=e} \log(D_k^i[e]) \right) \quad (37)$$

where N represents the number of nodes, $N_k = K$ is the count of latent factors, D_k^i is the distribution of nodes i and $D_k^i[e]$ denotes the probability that the generated embedding vector has label e . The indicator function $\mathbb{1}_{k=e}$ takes the value of one when the predicted label is correct.

4.6 Optimization

Finally, our aim is to learn the parameters θ of the inference model and ϕ of the regularization term for DVGA within a unified framework. By employing gradient descent, we optimize the combined objective function, which integrates the Evidence Lower Bound (ELBO) and the independence regularizer:

$$\min_{\theta, \phi} -\mathcal{L}_{ELBO}(\theta) + \lambda \mathcal{L}_{reg}(\phi), \quad (38)$$

Where λ is a hyper-parameter that controls the balance between $-\mathcal{L}_{ELBO}(\theta)$ and the impact of the regularizer. $\mathcal{L}_{reg}(\phi)$ is the loss of the discriminator mentioned above,

designed to encourage statistical independence among the disentangled node representations. The detailed training procedure for the DVGA model is illustrated in Algorithm 1.

Algorithm 1 The Training Procedure of DVGA

Input: Graph $G = (V, E, X)$, the number of disentangle layers L , the number of iterations T , the number of steps for flows M , affine coupling parameters of flows d' , convolution coefficients α and β , the number of channel K , latent dimension d , regularization parameter λ and training epochs E .

Parameters:

Weight matrix $W_k \in \mathbb{R}^{n \times \frac{d}{K}}$ for $k = 1, 2, \dots, K$;

Bias $b_k \in \mathbb{R}^{\frac{d}{K}}$ for $k = 1, 2, \dots, K$;

Scale parameters of neural network for flow $s_k : \mathbb{R}^{d'} \rightarrow \mathbb{R}^{d-d'}$ for $k = 1, 2, \dots, K$;

location parameters of neural network for flow $t_k : \mathbb{R}^{d'} \rightarrow \mathbb{R}^{d-d'}$ for $k = 1, 2, \dots, K$;

▷ All these parameters above are collectively denoted as θ ;

Parameters of a neural network $g_\phi : \mathbb{R}^{\frac{d}{K}} \rightarrow \mathbb{R}^K$.

- 1: **function** DGCN($G = (V, E, X), A$)
- 2: **for** $u \in V$ **do**
- 3: **for** $k = 1, 2, \dots, K$ **do** ▷ K channels.
- 4: $c_{u,k} \leftarrow \frac{W_k^\top x_u + b_k}{\|W_k^\top x_u + b_k\|_2}$.
- 5: **end for**
- 6: **end for**
- 7: **for** disentangle layer $l = 1, 2, \dots, L$ **do**
- 8: $z_{u,k}^{l-1} \leftarrow c_{u,k}, k = 1, 2, \dots, K, \forall u \in V$.

```

9:      for routing iteration  $t = 1, 2, \dots, T$  do
10:          Calculate  $p_{u,v}^{k,t-1}, q_{v,u}^{k,t-1}$  by Eqs. (16) and (17).
11:          Update the  $z_{u,k}^t, \forall u \in V$  by Eqs. (15) and (18).
12:      end for
13:           $c_{u,k} \leftarrow z_{u,k}^{t=L}$ ,  $k = 1, 2, \dots, K, \forall u \in V$ .            $\triangleright$  when  $l \leq L - 1$ .
14:  end for
15:   $z_u \leftarrow$  the concatenation of  $z_{u,1}, z_{u,2}, \dots, z_{u,K}$ .
16:   $Z \leftarrow$  each row represents the representation  $z_u$  of the node  $u, \forall u \in V$ .
17:  return  $Z$             $\triangleright$  disentangled representation.
18: end function
19: function ENCODER( $G = (V, E, X), A$ )
20:      $\mu = \text{DGCN}(G, A)$ ,
21:      $\log \sigma = \text{DGCN}(G, A)$ ,
22:      $\epsilon \sim \mathcal{N}(0, I)$ .
23:      $Z = \mu + \epsilon \circ \sigma$ .        $\triangleright$   $Z$  is assigned the value of  $\mu$  at test time. The symbol  $\circ$ 
denotes element-wise multiplication.
24:     return  $Z$ 
25: end function
26: function COMPONENT-WISE FLOW( $z_{u,k}$ )
27:     for  $m = 1, 2, \dots, M$  do
28:         Update  $z_{u,k}$  by Eqs. (20) and (21).
29:     end for
30:     return  $z_{u,k}$ 

```

```

31: end function
32: function DECODER( $Z$ )
33:    $Z_k \leftarrow$  the submatrix corresponding to the  $k$ -th channel in  $Z$ .
34:    $A_{factor}^k = \text{cos}(Z_k, Z_k) \in \mathbb{R}^{N \times N}$ .
35:    $\mathcal{D}(Z) \leftarrow \text{maxpooling}(A_{factor}^1, A_{factor}^2, \dots, A_{factor}^K)$ .
36:    $\hat{A} = \sigma(\mathcal{D}(Z) + ZZ^\top)$ .
37:   return  $\hat{A}$ 
38: end function
39: for epoch = 1 to  $E$  do
40:    $Z, D_{KL} = \text{ENCODER}(G, A)$ .
41:    $Z_k \leftarrow$  the submatrix corresponding to the  $k$ -th channel in  $Z$ .
42:    $Z_k = \text{COMPONENT-WISE FLOW}(\{z_{u,k}\})$ ,  $Z_k = \{z_{u,k}\}$ .
43:    $Z = \text{Stack}([Z_1, Z_2, \dots, Z_K], \text{dim}=0)$ .
44:    $p(A|Z) = \text{DECODER}(Z)$ .
45:   Calculate  $D_{KL}(q_\theta(Z|X, A) || \mathcal{N}(\mathbf{0}, \mathbf{I}))$  by Eq. (26).
46:   Calculate  $\mathcal{L}_{ELBO}(\theta)$  by Eq. (11) and the independence regularizer  $\mathcal{L}_{reg}(\phi)$  by
      Eq. (37).
47:   Update  $\theta$  and  $\phi$  to minimize  $\mathcal{L} = -\mathcal{L}_{ELBO}(\theta) + \lambda \mathcal{L}_{reg}(\phi)$  by Eq. (38) .
48: end for

```

For DGA, we employ the dynamic graph encoder in Section 4.1 to get latent representations, followed by the use of the factor-wise decoder in Eq. (22) for link prediction.

The corresponding loss is given by:

$$\min_{\theta, \phi} \mathcal{L}_{recon}(\theta) + \lambda \mathcal{L}_{reg}(\phi), \quad (39)$$

Where the first term corresponds to the reconstruction loss Eq. (13) for link prediction, typically implemented as a binary cross-entropy loss. The training process for the DGA model is outlined in Algorithm 2.

Algorithm 2 The Training Procedure of DGA

Input: Graph $G = (V, E, X)$, the number of disentangle layers L , the number of iterations T , convolution coefficients α and β , the number of channel K , latent dimension d , regularization parameter λ and training epochs E .

Parameters:

Weight matrix $W_k \in \mathbb{R}^{n \times \frac{d}{K}}$ for $k = 1, 2, \dots, K$;

Bias $b_k \in \mathbb{R}^{\frac{d}{K}}$ for $k = 1, 2, \dots, K$;

▷ All these parameters above are collectively denoted as θ ;

Parameters of a neural network $g_\phi : \mathbb{R}^{\frac{d}{K}} \rightarrow \mathbb{R}^K$.

- 1: **for** epoch = 1 to E **do**
 - 2: $Z, D_{KL} = \text{DGCN}(G, A)$.
 - 3: $p(A|Z) = \text{DECODER}(Z)$.
 - 4: Calculate $\mathcal{L}_{recon}(\theta)$ by Eq. (13) and the independence regularizer $\mathcal{L}_{reg}(\phi)$ by Eq. (37).
 - 5: Update θ and ϕ to minimize $\mathcal{L} = -\mathcal{L}_{recon}(\theta) + \lambda \mathcal{L}_{reg}(\phi)$ by Eq. (39).
 - 6: **end for**
-

5 Discussions

5.1 Time Complexity Analysis

We have conducted a theoretical analysis of the time complexity of the proposed DVGA model, which is $O((K^2 + fd + LT(C\frac{d}{K} + d))N + Md + (d + K)N^2) = O((K^2 + (f + LT)d + LTC)N + (d + K)N^2 + Md) = O(N^2)$. Here, N denotes the number of nodes in the graph, d is the dimensionality of latent variables, f represents the dimensionality of node input features, L is the number of layers in the disentangled layers employed by the dynamic disentangled graph encoder, K indicates the number of latent factors and T is the number of iterations for dynamic assignment. We define the maximum number of neighbors to be C . d, T, L, C and K are small constants. Specifically, the time complexity of our dynamic disentangled graph encoder is $O((fd + LT(c\frac{d}{K} + d))N)$. For the component-wise flow, K channels are required to be implemented, each with a dimension of $\frac{d}{K}$, and M steps, leading to a time complexity of $O(Md)$. The $O((d + K)N^2)$ is attributed to the factor-wise decoder, indicating that the computational cost is predominantly affected by the size of the graph-structured data, as demonstrated in the empirical study presented in Section 6.6. Nevertheless, we argue that our proposed DVGA remains reasonably efficient in practical applications, particularly when considering the substantial performance improvements validated in our experiments. The time complexity of computing the regularizer in our model is $O(NK^2)$. Similarly, we are able to get that the time complexity of DGA is $O((K^2 + fd + LT(C\frac{d}{K} + d))N + (d + K)N^2) = O((K^2 + (f + LT)d + LTC)N + (d + K)N^2) = O(N^2)$.

5.2 Number of Parameters Analysis

The number of parameters for the proposed DVGA is $O(fd + KMd'(d - d')) = O(fd + KMd^2)$, where N is the number of nodes, f represents the dimensionality of node input features, K is the number of latent factors, d is the dimensionality of latent variables and d' is employed in the affine coupling parameters of flows to determine the dimensions that remain unchanged from the previous step to the subsequent one. Specifically, the number of parameters for the dynamic disentangled encoder is $O(fd)$, the flow utilizes $O(KMd'(d - d'))$ parameters, and the independence regularization term involves $O(d)$ parameters. This parameter complexity is independent of the number of nodes and edges in the input graph, resulting in a relatively small value. Likewise, the number of parameters in DGA without utilizing flow is $O(fd)$.

6 Experiments

We show the performance of our proposed models and demonstrate their effectiveness in this section by presenting results on two unsupervised graph analytic tasks, including link prediction and node clustering. Additionally, our models are evaluated on a semi-supervised graph analytic task, namely, node classification. We also qualitatively investigate our models' performance in factor disentanglement. Further, we analyze the convergence behavior of our models and provide module ablation studies along with parameter sensitivity analysis.

6.1 Link prediction

Link prediction aims to predict whether there will be an edge or not between a pair of nodes (Loehlin, 2004). It stands as one of the most prevalent tasks in representation learning of network. Utilizing the decoder of our model, we can effectively recover lost links or predict potential links through an analysis of the given graph.

(1) **Real-World Datasets:** We assess our models performance on three widely used benchmark citation network datasets: Cora, CiteSeer, and PubMed, where nodes correspond to research papers, edges represent citations, and labels indicate the research areas (Sen et al., 2008). The features at the node level correspond to textual attributes found in the papers. Additionally, each node is assigned with a label indicating its class. We treat the graphs as undirected graphs. Table 1 provides a summary of the dataset statistics.

Table 1: Statistics for the citation network datasets.

Datasets	Cora	CiteSeer	PubMed
#Nodes	2708	3327	19717
#Edges	5429	4732	44338
#Features	1433	3703	500
#Classes	7	6	3

(2) **Synthetic Dataset:** To explore the performance of our models on graphs with m latent factors, we follow the methodology from Guo et al. (2022) for constructing synthetic graphs. Specifically, we create m Erdős-Rényi random graphs, each comprising 1000 nodes and 16 classes. Nodes are connected with a probability p within the

same class, and nodes are connected with a probability q within different classes. Subsequently, by summing their adjacency matrices, we aggregate these generated graphs and set elements greater than zero to one. Then, we get the final synthetic graph with m latent factors. This composite graph includes $16m$ classes, and assigns m labels to each node, derived from the original labels of m random graphs. Node representations are established based on the rows of the adjacency matrix. We fix the value of q at $3e^{-5}$ and fine-tune p to attain an average neighborhood size of around 40.

(3) **Baselines:** We evaluate the performance of DVGA and DGA in comparison to state-of-the-art baselines, including both graph embedding methods, such as Spectral Clustering (SC) (Tang et al., 2011), DeepWalk (Perozzi et al., 2014), and node2vec (Grover et al., 2016), as well as graph auto-encoder algorithms, including GAE/VGAE (Kipf et al., 2016a), ARG/ARVGA (Pan et al., 2018), LGAE/LVGAE (Salha et al., 2021), SIGVAE (Hasanzadeh et al., 2019) and GNAE/VGNAE (Ahn et al., 2021). Notably, SC, DeepWalk and node2vec lack the capability to use node features during the embedding learning process. Therefore, we evaluate them only on datasets without node features.

(4) **Evaluation metrics:** We employ two metrics, Area Under the ROC Curve (AUC) and Average Precision (AP), to evaluate performance (Kipf et al., 2016a). Each experiment is conducted five times, and the final scores are reported as mean values with standard errors. The real-world datasets are partitioned into training, testing, and validation sets. We augment the original graph with a balanced set of positive and negative (false) edges in the validation and testing sets. Specifically, the validation set comprises 5% edges, the test set includes 10% edges, and the remaining edges are used

for training. Both the validation and testing sets include an equal number of non-edges. For synthetic datasets, we perform a random split, allocating 60% to the training set, 20% to the validation set, and another 20% to the test set (Guo et al., 2022).

(5) **Parameter Settings:** We configure our DGA and DVGA models with $d = K\Delta d$, where d represents the hidden dimension, K denotes the number of channels, and $\Delta d = \frac{d}{K}$ is the output dimension of each channel. Hyper-parameter tuning is performed on the validation split of each dataset using Optuna (Akiba et al., 2019) for efficiency. Specifically, Optuna is executed for 100 trials for each configuration, and the hyper-parameter search space is defined as follows: dropout $\sim \{0, 0.05, \dots, 1\}$ with a step of 0.05, learning rate $\sim [1e^{-3}, 1]$, the number of channels $K \in \{2, 3, \dots, 10\}$, the iteration of routing $T \in \{1, 2, \dots, 10\}$, the number of layers $L \in \{1, 2, \dots, 6\}$, and the regularization term $\lambda \sim [1e^{-5}, 1]$. The output dimension of each channel is $\Delta d = 16$. For DVGA, the number of flow steps $\in \{1, 2, \dots, 5\}$. Using the best hyper-parameters, the models are trained for 3000 epochs, and the performance is reported based on five runs on the test split. Regarding the remaining baselines, we maintain consistency with our models in terms of the number of latent dimensions, while other parameters follow the configurations described in the corresponding papers.

(6) **Experimental Results:** Table 2 presents the results of link prediction on citation networks. As observed, DGA and DVGA consistently outperform other GAE-based or VGAE-based methods, which demonstrates the effectiveness of our models structure in generating more accurate predictions. This effectiveness results in substantial improvements in the performance of link prediction on real-world datasets. For instance, DVGA achieves a prediction accuracy increase of 2.1% and 0.5% when compared to

Table 2: Results for Link Prediction of citation networks. (* denotes dataset without features, i.e., $X = I$). Higher is better.

Model	Cora		CiteSeer		PubMed		Cora*		CiteSeer*		PubMed*	
	Auc	AP	Auc	AP	Auc	AP	Auc	AP	Auc	AP	Auc	AP
SC	-	-	-	-	-	-	89.4 ± 1.42	89.8 ± 1.44	90.1 ± 1.2	89.2 ± 1.31	90.1 ± 0.38	87.5 ± 0.65
DW	-	-	-	-	-	-	85 ± 1.29	86.4 ± 0.91	89 ± 0.99	90.6 ± 0.72	91.7 ± 0.11	92.2 ± 0.22
node2vec	-	-	-	-	-	-	85.7 ± 1.09	88.7 ± 1.27	90.3 ± 1.22	92.9 ± 0.74	93.9 ± 0.13	94.6 ± 0.15
GAE	91 ± 1.02	91.9 ± 0.89	90.1 ± 1.28	92 ± 0.96	96.6 ± 0.06	96.9 ± 0.04	83.8 ± 1.37	88.4 ± 0.74	76 ± 1.11	82.8 ± 0.56	81.2 ± 0.33	87.3 ± 0.27
LGAE	93.7 ± 0.38	94.5 ± 0.26	94.9 ± 0.88	95.4 ± 0.9	97.6 ± 0.08	97.7 ± 0.12	85 ± 1.21	89.4 ± 0.92	79.5 ± 1	84.9 ± 0.72	83.5 ± 0.45	88.5 ± 0.4
ARGA	93.1 ± 0.34	93.2 ± 0.44	93.9 ± 0.63	94.3 ± 0.65	91.1 ± 1.04	90.1 ± 1.08	76.4 ± 2.62	78 ± 2.11	71.5 ± 0.87	76.4 ± 0.76	79 ± 0.4	84.9 ± 0.38
GNAE	95 ± 0.34	95.6 ± 0.25	95.1 ± 0.48	96.1 ± 0.4	97.5 ± 0.11	97.4 ± 0.09	87 ± 1.26	91.1 ± 0.81	79.2 ± 1.2	85.2 ± 0.94	84.4 ± 0.13	89.8 ± 0.13
DGA	99.5 ± 0.11	99.6 ± 0.03	99.7 ± 0.17	99.7 ± 0.12	99.2 ± 0.04	99.2 ± 0.05	99.4 ± 0.13	99.5 ± 0.11	99.1 ± 0.07	99.2 ± 0.05	98.7 ± 0.13	98.8 ± 0.11
VGAE	90.9 ± 0.4	92.5 ± 0.28	89.2 ± 0.99	91.3 ± 0.55	95.7 ± 0.21	96 ± 0.2	84.8 ± 1.26	88.5 ± 0.85	76.4 ± 0.92	82.3 ± 0.47	82.3 ± 0.43	87.8 ± 0.29
LVGAE	94.7 ± 0.67	94.9 ± 0.82	94.9 ± 0.36	95.4 ± 0.35	97.6 ± 0.15	97.6 ± 0.23	84.8 ± 1.3	88.8 ± 0.98	79.1 ± 1.2	84.2 ± 0.91	84.1 ± 0.6	88.9 ± 0.42
ARVGA	91.1 ± 0.7	91.2 ± 0.74	91.9 ± 1.21	92.5 ± 1.13	95.4 ± 0.2	95.9 ± 0.1	68.9 ± 4.07	72.6 ± 3.59	71.4 ± 1.74	75.6 ± 2.23	84 ± 0.57	87.9 ± 0.48
SIGVAE	91.5 ± 0.68	92.6 ± 0.71	89.5 ± 0.82	91.4 ± 0.57	-	-	85.1 ± 0.8	88.5 ± 0.6	77.6 ± 1.58	83.4 ± 1.46	-	-
VGNAE	95.1 ± 1.27	95.6 ± 1.17	95.1 ± 0.54	96 ± 0.55	97.4 ± 0.15	97.4 ± 0.14	86 ± 0.97	90.1 ± 0.55	78.7 ± 1.46	85 ± 1.23	84.6 ± 0.44	89.7 ± 0.36
DVGA	97.1 ± 0.21	97.2 ± 0.18	95.6 ± 0.05	96.2 ± 0.12	97.6 ± 0.11	97.8 ± 0.06	97 ± 0.15	97.2 ± 0.21	94.6 ± 0.48	95.3 ± 0.37	97.8 ± 0.09	98 ± 0.07

Table 3: Results for Link Prediction of synthetic graphs with varying numbers of latent factors. (* denotes dataset without features, i.e., $X = I$). Higher is better.

Model	4		6		8		10	
	Auc	AP	Auc	AP	Auc	AP	Auc	AP
GAE	75.2 ± 1.24	73.2 ± 1.18	67.7 ± 0.61	66.4 ± 0.58	63.9 ± 0.34	62.2 ± 0.43	59.8 ± 0.25	57.9 ± 0.32
DGA	80.7 ± 1.04	81.8 ± 0.74	79.8 ± 1.04	81.3 ± 1.19	79.7 ± 0.96	80.6 ± 0.81	76.1 ± 1.7	79 ± 1.63
VGAE	74.8 ± 0.74	72.6 ± 0.64	58.4 ± 2.08	57.1 ± 2.04	55.9 ± 2.26	55 ± 1.94	51.6 ± 0.63	51.5 ± 0.84
DVGA	79.6 ± 1.61	83.6 ± 0.89	68.3 ± 1.94	74.5 ± 1.11	68.5 ± 1.43	72.7 ± 1.74	65.9 ± 1.87	70.5 ± 1.1

the best-performing VGAE-based baselines on Cora and CiteSeer, respectively. Similarly, DGA demonstrates prediction accuracy improvements of 4.7%, 4.8%, and 1.6% in terms of AUC against the strongest GAE-Based baselines on Cora, CiteSeer, and PubMed, respectively.

The formation processes of real-world graphs are typically unobservable, posing challenges in acquiring semantic information about latent factors. To further investigate the behavior of our models, as mentioned earlier before, we generate synthetic datasets. We present link prediction results in Table 3 with varying the number of channels (K) for latent factors. Our results indicate that our models consistently outperform baselines when varying the number of latent factors. Particularly, as the number of factors increases from 4 to 10, the performance of GAE and VGAE steadily decreases. In contrast, our model’s performance only exhibits a slight decrease, demonstrating its insensitivity to K . Especially, DVGA significantly outperforms VGAE by 27.3% in terms of AUC and 36.9% in terms of AP on the synthetic graph with ten latent factors.

These results arise from the limitations of existing methods in identifying the underlying latent factors crucial for exploring graph properties, thus hindering the learning

of disentangled representations. In contrast, our approach explicitly takes into account the entanglement of heterogeneous factors and designs a decoder specifically suited for this context. Consequently, in the task of link prediction, our method exhibits superior accuracy compared to other approaches across all three datasets.

6.2 Node clustering

In this section, we address the task of unsupervised node clustering in the graph. We utilize the K-means clustering algorithm on the learned node embeddings, setting K according to the number of classes specified in Table 1.

Table 4: Node clustering results on Cora and CiteSeer.

Model	Cora					CiteSeer				
	acc	precision	F1	NMI	ARI	acc	precision	F1	NMI	ARI
kmeans	0.148	0.317	0.168	0.183	0.109	0.235	0.233	0.206	0.097	0.073
SC	0.179	0.146	0.084	0.069	0.008	0.182	0.146	0.065	0.019	0.001
DW	0.469	0.614	0.510	0.413	0.331	0.417	0.591	0.439	0.208	0.142
GAE	0.286	0.315	0.283	0.386	0.318	0.356	0.469	0.364	0.125	0.058
VGAE	0.400	0.458	0.42	0.507	0.483	0.355	0.483	0.355	0.189	0.083
LGAE	0.313	0.343	0.325	0.488	0.388	0.386	0.479	0.423	0.332	0.262
LVGAE	0.395	0.446	0.407	0.500	0.451	0.346	0.429	0.359	0.363	0.306
ARGA	0.305	0.167	0.214	0.400	0.297	0.206	0.228	0.213	0.326	0.299
ARVGA	0.281	0.325	0.299	0.517	0.475	0.322	0.403	0.352	0.287	0.242
GNAE	0.197	0.298	0.223	0.523	0.475	0.407	0.676	0.426	0.266	0.073
VGNAE	0.289	0.329	0.303	0.515	0.466	0.293	0.326	0.305	0.304	0.255
DGA	0.698	0.786	0.714	0.526	0.479	0.521	0.606	0.524	0.295	0.211
DVGA	0.738	0.766	0.744	0.514	0.508	0.608	0.700	0.640	0.372	0.341

(1) **Evaluation metrics:** The node labels provided in Table 1 serve as the true clus-

tering labels for our evaluation. We adopt the approach introduced in Xia et al. (2014), where we initially use the Munkres assignment algorithm (Munkres , 1957) to match the predicted labels with the true labels. Subsequently, we employ five metrics for validating the clustering results, specifically reporting (i) accuracy (acc); (ii) precision; (iii) F1-score (F1); (iv) normalized mutual information (NMI); (v) average rand index (ARI). Consistent with previous studies such as Pan et al. (2018) and Shi et al. (2020), our focus is only on Cora and CiteSeer.

(2) **Experimental Results:** Table 4 shows the results of node clustering for Cora and CiteSeer. The results indicate that both DGA and DVGA exhibit a substantial enhancement across all five metrics in comparison to the remaining baseline methods. For instance, on CiteSeer, DVGA has demonstrated a 49.4% accuracy improvement compared to GNAE and a 45.8% improvement compared to DW. Additionally, it has achieved a 2.5% increase in NMI compared to LVGAE and a 78.8% increase compared to DW. On Cora, DGA has exhibited a 71.6% precision enhancement compared to VGAE and a 28.0% improvement compared to DW. Furthermore, it has shown a 0.6% increase in NMI compared to GNAE and a 27.4% improvement compared to DW. This results further proved the effectiveness and superiority of our model.

6.3 Semi-supervised node classification

The node classification task aims to predict the labels of the remaining nodes by utilizing the labels of a subset of nodes in the underlying graph. We adapt DGA and DVGA for node classification on three citation networks by adjusting the loss function to incorporate both the original model loss and a semi-supervised classification term. A

hyper-parameter is introduced to control the relative importance of components in the combined objective function. We employ an additional fully-connected neural network to map the latent representations to softmax probabilities for the required number of classes. During the optimization process, all parameters are trained jointly.

Table 5: Classification accuracies (in percent). Baseline results from Kipf et al. (2016b).

Model	Cora	CiteSeer	PubMed
ManiReg	59.5	60.1	70.7
SemeEmb	59	59.6	71.1
LP	68	45.3	63
DeepWalk	67.2	43.2	65.3
ICA	75.1	69.1	73.9
Planetoid	75.7	64.7	77.2
GCN	81.5	70.3	79
DGA	80.8	70.2	79.5
DVGA	81.9	65.6	80.9

Experimental Results: The results of node classification are summarized in Table 5. We observe that our models outperform other competing models on Cora and PubMed. It also shows comparable performance to CiteSeer, where it closely aligns with the GCN, considered the best baseline. The competitive performance in comparison to state-of-the-art methods highlights the robust capabilities of our model, even though it is not specifically trained for this task.

6.4 Qualitative Evaluation

For a more comprehensive understanding of our proposed models, we conduct two qualitative experiments for a thorough examination in parallel with VGAE. These evaluations focus on performance of disentanglement and the informativeness learned in

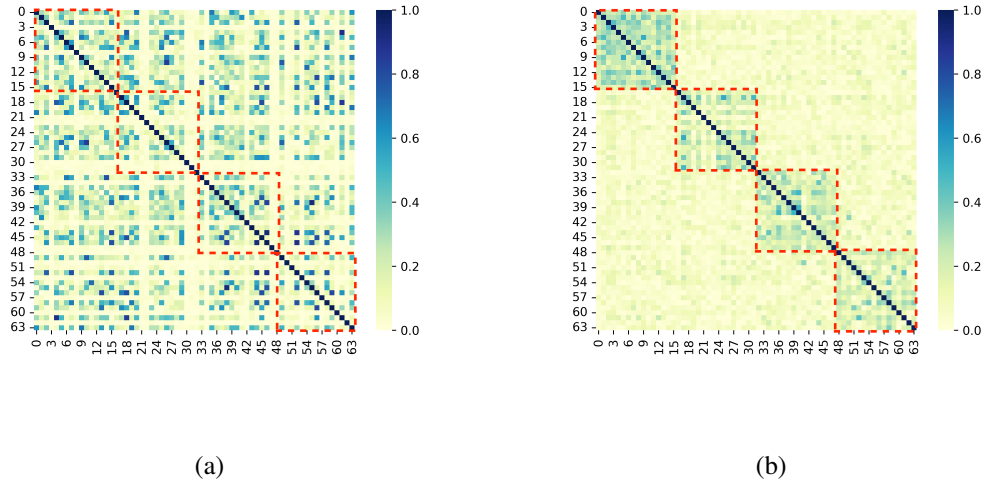
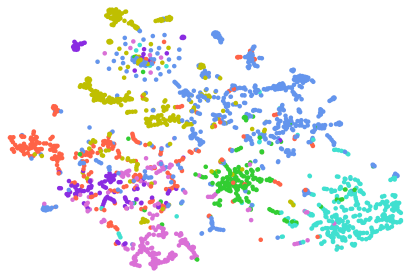


Figure 3: The absolute correlation values between the elements of the 64-dimensional representations learned by VGAE and DVGA on a synthetic graph with four latent factors. DVGA shows clearly four diagonal blocks (marked by the red dashed blocks), but VGAE does not show this correlation.

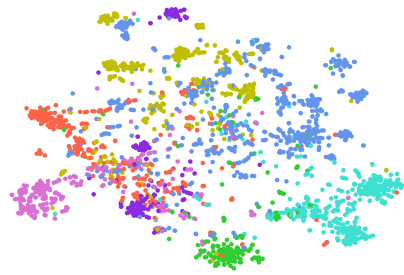
the embeddings.

(1) **Correlation of Latent Features:** We plot the correlation of the dimensions of latent features on the synthetic graph with four latent factors in Figure 3. The figure illustrates the absolute correlation values between elements within the 64-dimensional graph representations obtained from VGAE and DVGA. DVGA’s correlation plot exhibits a clear blockwise correlation pattern, specifically with four distinct diagonal blocks. This suggests that the four channels in DVGA are likely to capture mutually exclusive information. Therefore, our proposed method successfully learns disentangled node embeddings and captures the latent factors leading to connections to some degree. This will provide interpretability for the link prediction results.

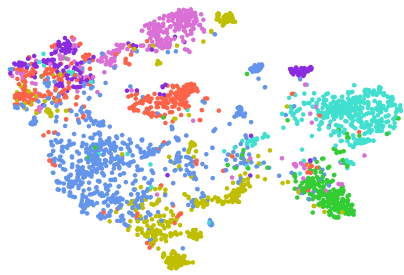
(2) **Visualization of Node Embeddings:** Figure 4 provides a visual comparison of



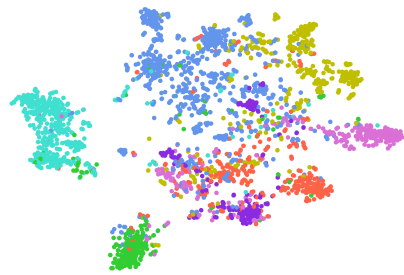
(a) DW



(b) VGAE



(c) ARVGA



(d) DVGA

Figure 4: Visualization of node embeddings on Cora.

the learned node embeddings from DW, VGAE, ARVGA, and DVGA on Cora. Utilizing t-SNE (Van et al., 2008), we project the node representations into a two-dimensional space. It is evident that DVGA generally learns superior node embeddings, showcasing high intraclass similarity and interclass differences. These findings emphasize the effectiveness of DVGA in learning disentangled representations of graph-structured data.

Table 6: Ablation Studies of DGA.

Model	Cora		CiteSeer		PubMed	
	Auc	AP	Auc	AP	Auc	AP
<i>w/o indep</i>	99.2 ± 0.08	99.1 ± 0.15	99.3 ± 0.1	99.2 ± 0.09	98.4 ± 0.02	98.3 ± 0.01
<i>w/o disen</i>	98.9 ± 0.19	98.8 ± 0.15	99.0 ± 0.21	98.7 ± 0.24	99.0 ± 0.1	98.9 ± 0.1
DGA	99.5 ± 0.11	99.6 ± 0.03	99.7 ± 0.17	99.7 ± 0.12	99.2 ± 0.04	99.2 ± 0.05

Table 7: Ablation Studies of DVGA.

Model	Cora		CiteSeer		PubMed	
	Auc	AP	Auc	AP	Auc	AP
<i>w/o flow</i>	92.5 ± 0.23	92.7 ± 0.78	90.1 ± 1.05	91.3 ± 0.95	91.7 ± 0.05	92.7 ± 0.14
<i>w/o indep</i>	97.0 ± 0.07	97.2 ± 0.09	94.7 ± 0.16	95.3 ± 0.33	97.7 ± 0.01	97.9 ± 0.02
<i>w/o disen</i>	90.4 ± 0.41	91.1 ± 0.41	87.7 ± 0.88	89.0 ± 0.72	89.8 ± 0.3	91.2 ± 0.34
DVGA	97.1 ± 0.21	97.2 ± 0.18	95.6 ± 0.05	96.2 ± 0.12	97.6 ± 0.11	97.8 ± 0.06

6.5 Analysis

(1) **Ablation Studies:** We conduct ablation studies on the essential components of our models to validate their contributions. We compare DVGA with the following three

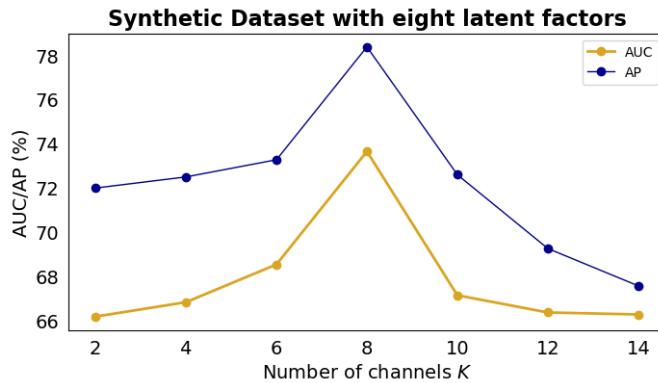


Figure 5: Results for link prediction of synthetic graphs with different number of channels K .

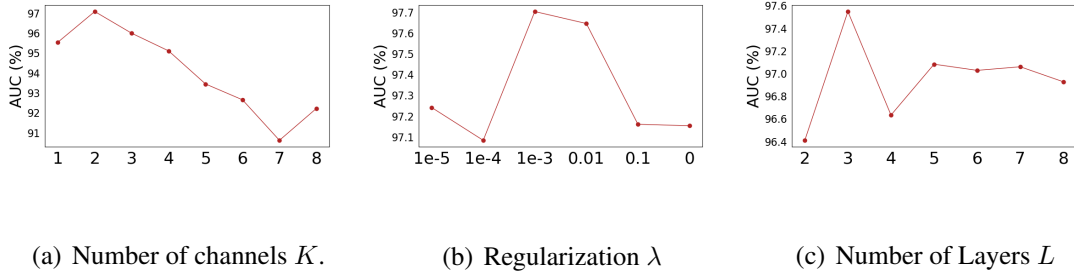


Figure 6: Analysis of different hyper-parameters in terms of AUC on Cora.

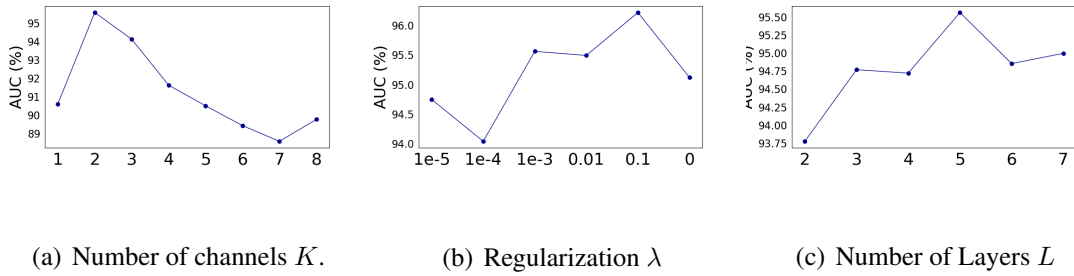


Figure 7: Analysis of different hyper-parameters in terms of AUC on CiteSeer.

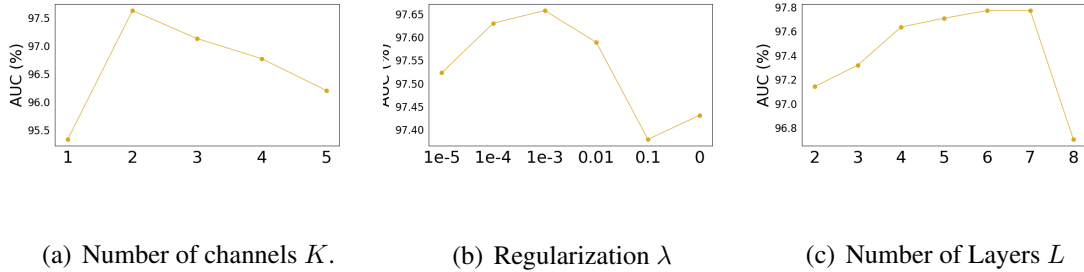


Figure 8: Analysis of different hyper-parameters in terms of AUC on PubMed.

variants: (1) *w/o* flow: i.e., setting $M = 0$. (2) *w/o* indep: i.e., setting $\lambda = 0$. (3) *w/o* disen: i.e., setting $K = 1$, and in this case, our method degenerates into the traditional entangled variational graph auto-encoder. For DGA, as it lacks the flow component in its structure, we consider its similar variants *w/o* indep and *w/o* disen. For simplicity, we only report the results of the unsupervised link prediction task, with similar patterns observed in other tasks.

The results for DGA, DVGA, and their variants are presented in Tables 6 and 7. It is evident that removing any module diminishes the predictive capability of the models across all datasets. Especially noteworthy is the substantial impact of eliminating the disentanglement mechanism, as observed in the significant reduction in model performance. For instance, the results of DVGA on Cora illustrate this effect. Therefore, we conclude that each module we designed contributes significantly to the models' capability, and their presence collectively enhances the predictive power of the models.

(2) **Hyper-Parameter Sensitivity:** We explore the sensitivity of three crucial hyperparameters. We present the results for evaluating the channel K on synthetic datasets (Figure 5) and the results for all three hyperparameters on Cora (Figure 6), CiteSeer (Figure 7), and PubMed (Figure 8), with the number of channels K recognized as the most significant one. Here, we present the results of DVGA under the AUC metric for link prediction. Similar findings are observed for the AP metric, as illustrated in Figures 10, 11, and 12 in Appendix.

A) *Number of channels K :* We initially examine K on the synthetic dataset with eight latent factors. It can be seen that the performance initially increases with an increment in K , reaching its peak at $K = 8$, and subsequently decreases. This suggests that an optimal K aligning with the ground-truth latent factors outputs the best results. It also illustrates that our model learns representations that promote disentanglement and are effective for node-related tasks. Then we investigate the impact of the channel K in three citation networks. As observed previously, the performance initially increases, then reaches a peak before experiencing a notable declining. This pattern also shows that an appropriate number

of channels K , matching the real number of latent factors can result in improved performance;

B) *Regularization coefficient λ* : The regularization coefficient λ can affect the model’s performance. A large λ tends to excessively emphasize the independence between the latent factors, whereas an excessively small λ constrains the influence of the independence regularization. Through empirical observation, we find that setting λ to 0.01, 0.1, and 0.001 respectively leads to satisfactory results for Cora, CiteSeer, and PubMed.

C) *Number of disentangle layers L* : The significance of the number of disentangle layers L lies in the fact that a model with a small L exhibits restricted capacity, potentially hindering its ability to integrate sufficient information from neighbors. From the graphs, we observe that for Cora, the optimal L is 3; for CiteSeer, it is 5; and for PubMed, it is 7. Additionally, when L is too large, there is a decline in predictive capability, suggesting that excessive message propagation can result in overfitting, thereby compromising model performance;

6.6 Convergence Behavior and Complexity Analysis

Figure 9 shows the evolution of testing AUC for DVGA and VGAE. Similar results regarding AP are depicted in Figure 13 in Appendix. As observed from the figure, VGAE tends to easily fall into local optima, while our model exhibits greater stability, converging to higher peaks. Regarding computational complexity, Table 8 presents the time taken for training in each epoch. DVGA is slower on three citation network datasets

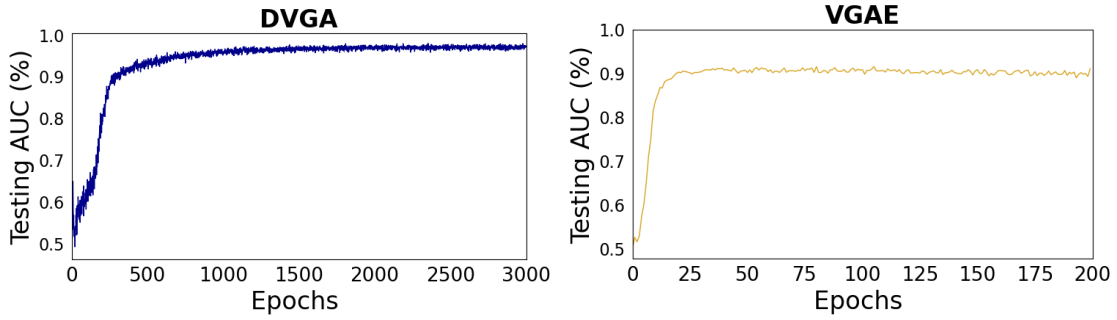
compared to VGAE, mainly because of the computation of the graph with a complexity of $O(N^2)$. Nevertheless, considering significant enhancement in performance, we believe these costs are worthwhile, particularly with the enhancement in computational capabilities and stability.

Table 8: Average training time (s) per epoch.

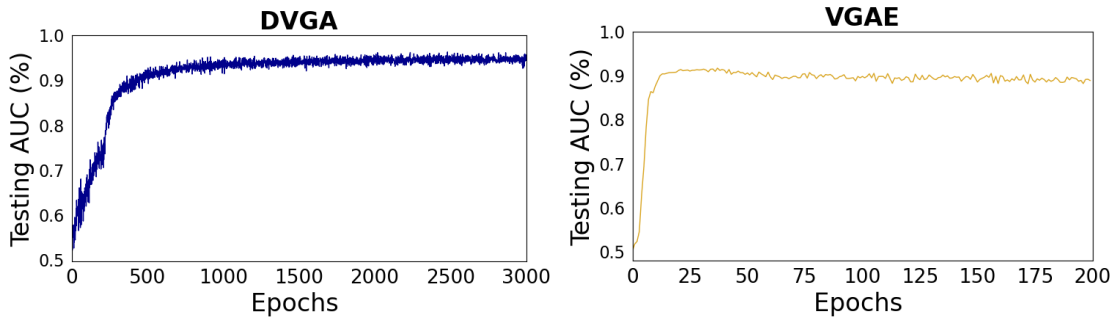
Model	Cora	CiteSeer	PubMed
VGAE	0.144	0.167	1.716
DVGA	0.296	0.341	3.635

7 Conclusion

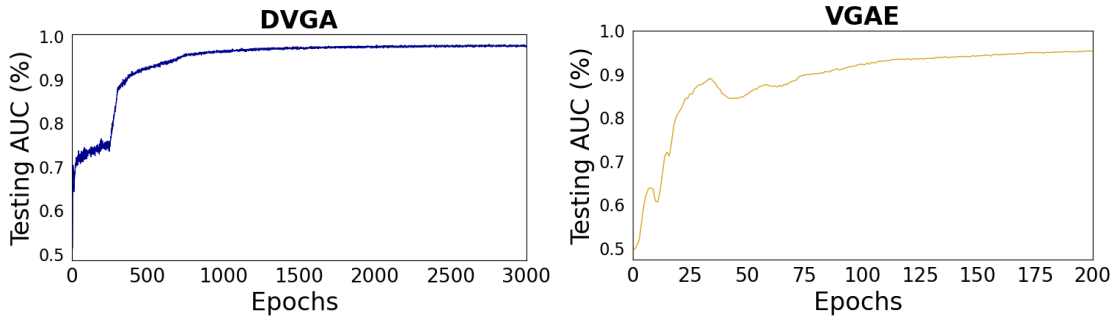
In this article, we investigate the problem of learning disentangled network representations using generative models and propose the Disentangled Graph Auto-Encoder (DGA) and Disentangled Variational Graph Auto-Encoder (DVGA) models. We design a dynamic disentangled graph encoder capable of aggregating features in a disentangled manner. Additionally, we introduce component-wise flow for the DVGA, encouraging DVGA to learn expressive representations that best describe graphs. We also propose a factor-wise decoder tailored for disentangled representations to improve its ability to predict graph structures. Independent regularization is introduced to eliminate statistical dependencies between different latent representations. Empirical results including quantitative and qualitative experiments on synthetic and real-world datasets demonstrate the effectiveness of our method in learning interpretable disentangled representations. As for future work, exploring new applications that leverage the robustness and interpretability brought by disentangled representations will be an interesting and promising research direction.



(a) Cora



(b) CiteSeer



(c) PubMed

Figure 9: The convergence behavior of VGAE and our proposed DVGA on the test set for the link prediction task in terms of AUC. (a) Cora. (b) CiteSeer. (c) PubMed.

Acknowledgments

This work was funded by the National Nature Science Foundation of China under Grant No. 12320101001 and 12071428.

Appendix

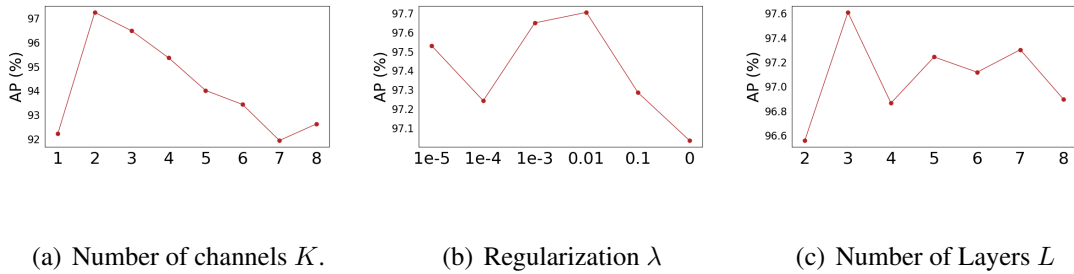


Figure 10: Analysis of different hyper-parameters in terms of AP on Cora.

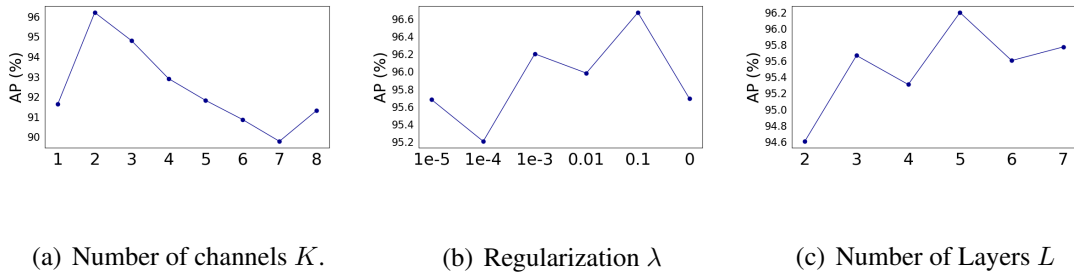


Figure 11: Analysis of different hyper-parameters in terms of AP on CiteSeer.

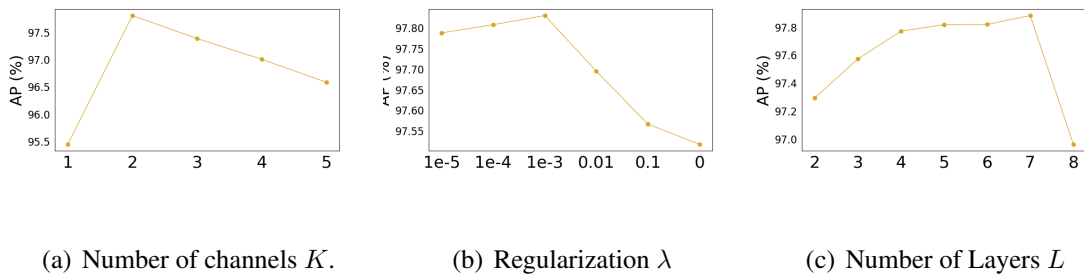
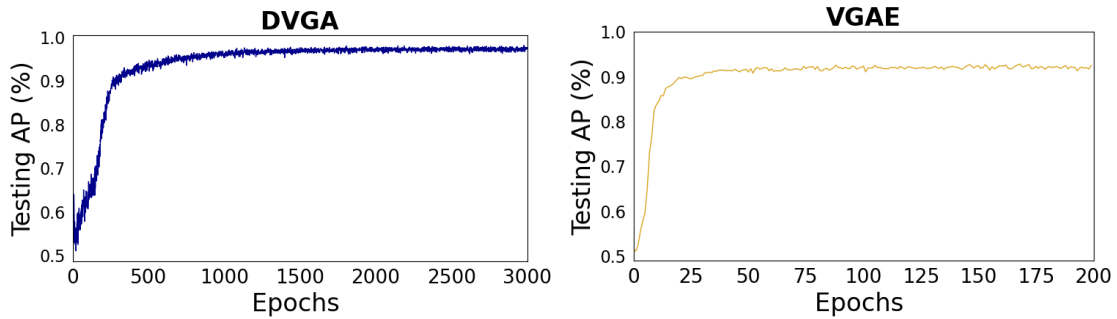
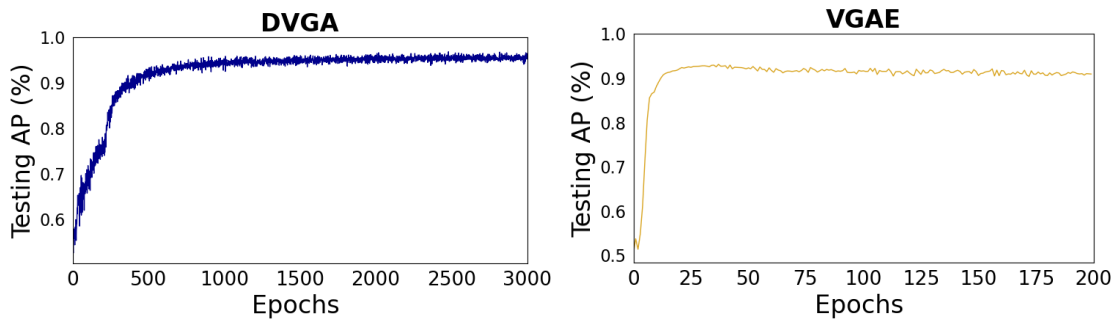


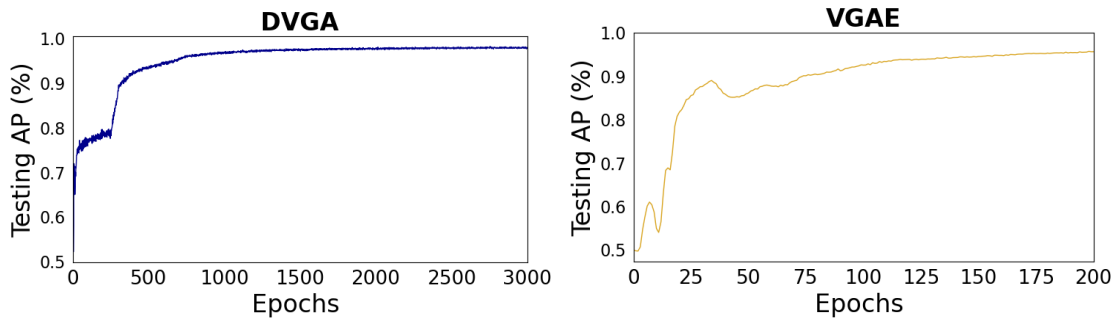
Figure 12: Analysis of different hyper-parameters in terms of AP on PubMed.



(a) Cora



(b) CiteSeer



(c) PubMed

Figure 13: The convergence behavior of VGAE and our proposed DVGA on the test set for the link prediction task in terms of AP. (a) Cora. (b) CiteSeer. (c) PubMed.

References

Akiba, T., Sano, S., Yanase, T., Ohta, T., & Koyama, M. (2019). Optuna: A next-generation hyper-parameter optimization framework. *In Proceedings of the 25th*

- ACM SIGKDD international conference on knowledge discovery & data mining (pp. 2623-2631).*
- Ahn, S. J., & Kim, M. (2021). Variational graph normalized autoencoders. *In Proceedings of the 30th ACM international conference on information & knowledge management (pp. 2827-2831).*
- Bhagat, S., Cormode, G., & Muthukrishnan, S. (2011). Node classification in social networks. *Social network data analytics, 115-148.*
- Bengio, Y., Courville, A., & Vincent, P. (2013). Representation learning: A review and new perspectives. *IEEE transactions on pattern analysis and machine intelligence, 35(8)*, 1798-1828.
- Burgess, C. P., Higgins, I., Pal, A., Matthey, L., Watters, N., Desjardins, G., & Lerchner, A. (2018). Understanding disentangling in β -VAE. *arXiv preprint arXiv:1804.03599.*
- Brody, S., Alon, U., & Yahav, E. (2021). How attentive are graph attention networks? *arXiv preprint arXiv:2105.14491.*
- Bouritsas, G., Frasca, F., Zafeiriou, S., & Bronstein, M. M. (2022). Improving graph neural network expressivity via subgraph isomorphism counting. *IEEE Transactions on Pattern Analysis and Machine Intelligence, 45(1)*, 657-668.
- Cao, S., Lu, W., & Xu, Q. (2016). Deep neural networks for learning graph representations. *In Proceedings of the AAAI conference on artificial intelligence (Vol. 30, No. 1).*

- Cai, H., Zheng, V. W., & Chang, K. C. C. (2018). A comprehensive survey of graph embedding: Problems, techniques, and applications. *IEEE transactions on knowledge and data engineering*, 30(9), 1616-1637.
- Chen, R. T., Li, X., Grosse, R. B., & Duvenaud, D. K. (2018). Isolating sources of disentanglement in variational autoencoders. *Advances in neural information processing systems*, 31.
- Davidson, T. R., Falorsi, L., De Cao, N., Kipf, T., & Tomczak, J. M. (2018). Hyper-spherical variational auto-encoders. *arXiv preprint arXiv:1804.00891*.
- Doersch, C. (2016). Tutorial on variational autoencoders. *arXiv preprint arXiv:1606.05908*.
- Daud, N. N., Ab Hamid, S. H., Saadoon, M., Sahran, F., & Anuar, N. B. (2020). Applications of link prediction in social networks: A review. *Journal of Network and Computer Applications*, 166, 102716.
- Fu, J., Zhang, X., Li, S., & Chen, D. (2023). Variational Disentangled Graph Auto-Encoders for Link Prediction. *arXiv preprint arXiv:2306.11315*.
- Grover, A., & Leskovec, J. (2016). node2vec: Scalable feature learning for networks. *In Proceedings of the 22nd ACM SIGKDD international conference on Knowledge discovery and data mining (pp. 855-864)*.
- Goyal, P., & Ferrara, E. (2018). Graph embedding techniques, applications, and performance: A survey. *Knowledge-Based Systems*, 151, 78-94.

- Grover, A., Zweig, A., & Ermon, S. (2019). Graphite: Iterative generative modeling of graphs. *In International conference on machine learning (pp. 2434-2444)*. PMLR.
- Geng, Y., Chen, J., Zhang, W., Xu, Y., Chen, Z., Z. Pan, J., ... & Chen, H. (2022). Disentangled ontology embedding for zero-shot learning. *In Proceedings of the 28th ACM SIGKDD conference on knowledge discovery and data mining (pp. 443-453)*.
- Guo, J., Huang, K., Yi, X., & Zhang, R. (2022). Learning disentangled graph convolutional networks locally and globally. *IEEE Transactions on Neural Networks and Learning Systems*.
- He, K., Zhang, X., Ren, S., & Sun, J. (2016). Deep residual learning for image recognition. *In Proceedings of the IEEE conference on computer vision and pattern recognition (pp. 770-778)*.
- Higgins, I., Matthey, L., Pal, A., Burgess, C., Glorot, X., Botvinick, M., ... & Lerchner, A. (2016). beta-vae: Learning basic visual concepts with a constrained variational framework. *In International conference on learning representations*.
- Hamilton, W. L., Ying, R., & Leskovec, J. (2017). Representation learning on graphs: Methods and applications. *arXiv preprint arXiv:1709.05584*.
- Hamilton, W., Ying, Z., & Leskovec, J. (2017). Inductive representation learning on large graphs. *Advances in neural information processing systems*, 30.
- Higgins, I., Amos, D., Pfau, D., Racaniere, S., Matthey, L., Rezende, D., & Lerchner, A. (2018). Towards a definition of disentangled representations. *arXiv preprint arXiv:1812.02230*.

- Hasanzadeh, A., Hajiramezanali, E., Narayanan, K., Duffield, N., Zhou, M., & Qian, X. (2019). Semi-implicit graph variational auto-encoders. *Advances in neural information processing systems*, 32.
- Kullback, S., & Leibler, R. A. (1951). On information and sufficiency. *The annals of mathematical statistics*, 22(1), 79-86.
- Kingma, D. P., & Welling, M. (2013). Auto-encoding variational bayes. *arXiv preprint arXiv:1312.6114*.
- Kipf, T. N., & Welling, M. (2016a). Variational graph auto-encoders. *arXiv preprint arXiv:1611.07308*.
- Kipf, T. N., & Welling, M. (2016b). Semi-Supervised Classification with Graph Convolutional Networks. *International Conference on Learning Representations*.
- Kim, H., & Mnih, A. (2018). Disentangling by factorising. *In International Conference on Machine Learning (pp. 2649-2658)*. PMLR.
- Kim, M., Wang, Y., Sahu, P., & Pavlovic, V. (2019). Relevance factor vae: Learning and identifying disentangled factors. *arXiv preprint arXiv:1902.01568*.
- Khan, R. A., Anwaar, M. U., & Kleinsteuber, M. (2021). Epitomic variational graph autoencoder. *In 2020 25th International Conference on Pattern Recognition (ICPR) (pp. 7203-7210)*. IEEE.
- Loehlin, J. C. (2004). Latent variable models: An introduction to factor, path, and structural equation analysis. *Lawrence Erlbaum Associates Publishers*, 2004.

- Liu, Y., Wang, X., Wu, S., & Xiao, Z. (2020). Independence promoted graph disentangled networks. *In Proceedings of the AAAI Conference on Artificial Intelligence (Vol. 34, No. 04, pp. 4916-4923)*.
- Locatello, F., Poole, B., Rätsch, G., Schölkopf, B., Bachem, O., & Tschannen, M. (2020). Weakly-supervised disentanglement without compromises. *In International Conference on Machine Learning (pp. 6348-6359)*. PMLR.
- Li, H., Wang, X., Zhang, Z., Yuan, Z., Li, H., & Zhu, W. (2021). Disentangled contrastive learning on graphs. *Advances in Neural Information Processing Systems, 34, 21872-21884*.
- Li, D., Li, D., & Lian, G. (2023). Variational Graph Autoencoder with Adversarial Mutual Information Learning for Network Representation Learning. *ACM Transactions on Knowledge Discovery from Data, 17(3), 1-18*.
- Luan, S., Hua, C., Xu, M., Lu, Q., Zhu, J., Chang, X. W., ... & Precup, D. (2023). When do graph neural networks help with node classification: Investigating the homophily principle on node distinguishability. *arXiv preprint arXiv:2304.14274*.
- Munkres, J. (1957). Algorithms for the assignment and transportation problems. *Journal of the society for industrial and applied mathematics, 5(1), 32-38*.
- Ma, J., Cui, P., Kuang, K., Wang, X., & Zhu, W. (2019). Disentangled graph convolutional networks. *In International conference on machine learning (pp. 4212-4221)*. PMLR.

- Ou, M., Cui, P., Pei, J., Zhang, Z., & Zhu, W. (2016). Asymmetric transitivity preserving graph embedding. *In Proceedings of the 22nd ACM SIGKDD international conference on Knowledge discovery and data mining (pp. 1105-1114)*.
- Perozzi, B., Al-Rfou, R., & Skiena, S. (2014). Deepwalk: Online learning of social representations. *In Proceedings of the 20th ACM SIGKDD international conference on Knowledge discovery and data mining (pp. 701-710)*.
- Papamakarios, G., Pavlakou, T., & Murray, I. (2017). Masked autoregressive flow for density estimation. *Advances in neural information processing systems*, 30.
- Pan, S., Hu, R., Long, G., Jiang, J., Yao, L., & Zhang, C. (2018). Adversarially regularized graph autoencoder for graph embedding. *arXiv preprint arXiv:1802.04407*.
- Sen, P., Namata, G., Bilgic, M., Getoor, L., Galligher, B., & Eliassi-Rad, T. (2008). Collective classification in network data. *AI magazine*, 29(3), 93-106.
- Simonovsky, M., & Komodakis, N. (2018). Graphvae: Towards generation of small graphs using variational autoencoders. *In Artificial Neural Networks and Machine Learning—ICANN 2018: 27th International Conference on Artificial Neural Networks, Rhodes, Greece, October 4-7, 2018, Proceedings, Part I 27 (pp. 412-422)*. Springer International Publishing.
- Shan, H., Jin, D., Jiao, P., Liu, Z., Li, B., & Huang, Y. (2020). NF-VGA: Incorporating Normalizing Flows into Graph Variational Autoencoder for Embedding Attribute Networks. *In 2020 IEEE International Conference on Data Mining (ICDM) (pp. 1244-1249)*. IEEE.

- Shi, H., Fan, H., & Kwok, J. T. (2020). Effective decoding in graph auto-encoder using triadic closure. *In Proceedings of the AAAI Conference on Artificial Intelligence (Vol. 34, No. 01, pp. 906-913).*
- Salha, G., Hennequin, R., & Vazirgiannis, M. (2021). Simple and effective graph autoencoders with one-hop linear models. *In Machine Learning and Knowledge Discovery in Databases: European Conference, ECML PKDD 2020, Ghent, Belgium, September 14–18, 2020, Proceedings, Part I (pp. 319-334). Springer International Publishing.*
- Sun, L., Liu, X., Zhao, M., & Yang, B. (2021). Interpretable Variational Graph Autoencoder with Noninformative Prior. *Future Internet, 13(2), 51.*
- Shen, X., Liu, F., Dong, H., Lian, Q., Chen, Z., & Zhang, T. (2022). Weakly supervised disentangled generative causal representation learning. *The Journal of Machine Learning Research, 23(1), 10994-11048.*
- Son, J., & Kim, D. (2023). Applying network link prediction in drug discovery: an overview of the literature. *Expert Opinion on Drug Discovery, 1-14.*
- Tang, L., & Liu, H. (2011). Leveraging social media networks for classification. *Data Mining and Knowledge Discovery, 23, 447-478.*
- Tang, J., Qu, M., Wang, M., Zhang, M., Yan, J., & Mei, Q. (2015). Line: Large-scale information network embedding. *In Proceedings of the 24th international conference on world wide web (pp. 1067-1077).*
- Träuble, F., Creager, E., Kilbertus, N., Locatello, F., Dittadi, A., Goyal, A., ... & Bauer,

- S. (2021). On disentangled representations learned from correlated data. *In International Conference on Machine Learning (pp. 10401-10412)*. PMLR.
- Tsitsulin, A., Palowitch, J., Perozzi, B., & Müller, E. (2023). Graph clustering with graph neural networks. *Journal of Machine Learning Research, 24(127)*, 1-21.
- Van der Maaten, L., & Hinton, G. (2008). Visualizing data using t-SNE. *Journal of machine learning research, 9(11)*.
- Veličković, P., Cucurull, G., Casanova, A., Romero, A., Lio, P., & Bengio, Y. (2017). Graph attention networks. *arXiv preprint arXiv:1710.10903*.
- Weisstein, E. W. (2006). Jensen's inequality. *MathWorld—A Wolfram Web Resource*.
- Wang, Z., Chen, C., & Li, W. (2017). Predictive network representation learning for link prediction. *Proceedings of the 40th international ACM SIGIR conference on research and development in information retrieval (pp. 969-972)*.
- Wang, D., Cui, P., & Zhu, W. (2016). Structural deep network embedding. *In Proceedings of the 22nd ACM SIGKDD international conference on Knowledge discovery and data mining (pp. 1225-1234)*.
- Wang, X., Cui, P., Wang, J., Pei, J., Zhu, W., & Yang, S. (2017). Community preserving network embedding. *In Proceedings of the AAAI conference on artificial intelligence (Vol. 31, No. 1)*.
- Wang, Y., Tang, S., Lei, Y., Song, W., Wang, S., & Zhang, M. (2020). Disenhan: Disentangled heterogeneous graph attention network for recommendation. *In Proceedings*

of the 29th ACM international conference on information & knowledge management (pp. 1605-1614).

Wang, M., Qiu, L., & Wang, X. (2021). A survey on knowledge graph embeddings for link prediction. *Symmetry*, *13*(3), 485.

Wang, C., Pan, S., Long, G., Zhu, X., & Jiang, J. (2017). Mgae: Marginalized graph autoencoder for graph clustering. *In Proceedings of the 2017 ACM on Conference on Information and Knowledge Management (pp. 889-898).*

Wu, J., Shi, W., Cao, X., Chen, J., Lei, W., Zhang, F., ... & He, X. (2021). DisenKGAT: knowledge graph embedding with disentangled graph attention network. *In Proceedings of the 30th ACM international conference on information & knowledge management (pp. 2140-2149).*

Wu, L., Li, Z., Zhao, H., Liu, Q., Wang, J., Zhang, M., & Chen, E. (2021). Learning the implicit semantic representation on graph-structured data. *In Database Systems for Advanced Applications: 26th International Conference, DASFAA 2021, Taipei, Taiwan, April 11–14, 2021, Proceedings, Part I 26 (pp. 3-19). Springer International Publishing.*

Wang, X., Bo, D., Shi, C., Fan, S., Ye, Y., & Philip, S. Y. (2022). A survey on heterogeneous graph embedding: methods, techniques, applications and sources. *IEEE Transactions on Big Data*, *9*(2), 415-436.

Wu, L., Lin, H., Xia, J., Tan, C., & Li, S. Z. (2022). Multi-level disentanglement graph

- neural network. *Neural Computing and Applications*, 34(11), 9087-9101. *Neural Computing and Applications*, 34(11), 9087-9101.
- Xia, R., Pan, Y., Du, L., & Yin, J. (2014). Robust multi-view spectral clustering via low-rank and sparse decomposition. *In Proceedings of the AAAI conference on artificial intelligence (Vol. 28, No. 1)*.
- Xingyi Zhang, Kun Xie, Sibowang, and Zengfeng Huang. 2021. Learning Based Proximity Matrix Factorization for Node Embedding. *In Proceedings of the 27th ACM SIGKDD Conference on Knowledge Discovery & Data Mining*. 2243–2253.
- Xiao, T., Chen, Z., Guo, Z., Zhuang, Z., & Wang, S. (2022). Decoupled self-supervised learning for graphs. *Advances in Neural Information Processing Systems*, 35, 620-634.
- Xiao, S., Wang, S., Dai, Y., & Guo, W. (2022). Graph neural networks in node classification: survey and evaluation. *Machine Vision and Applications*, 33, 1-19.
- Yang, C., Liu, Z., Zhao, D., Sun, M., & Chang, E. Y. (2015). Network representation learning with rich text information. *In IJCAI (Vol. 2015, pp. 2111-2117)*.
- Yang, Y., Feng, Z., Song, M., & Wang, X. (2020). Factorizable graph convolutional networks. *Advances in Neural Information Processing Systems*, 33, 20286-20296.
- Zhang, D., Yin, J., Zhu, X., & Zhang, C. (2017). User profile preserving social network embedding. *In IJCAI International Joint Conference on Artificial Intelligence*.
- Zaiqiao Meng, Shangsong Liang, Hongyan Bao, and Xiangliang Zhang. 2019. Co-

embedding attributed networks. *In Proceedings of the twelfth ACM international conference on web search and data mining*. 393–401.

Zheng, S., Zhu, Z., Liu, Z., Ji, S., Cheng, J., & Zhao, Y. (2021). Adversarial graph disentanglement. *arXiv preprint arXiv:2103.07295*.

Zhao, T., Zhang, X., & Wang, S. (2022). Exploring edge disentanglement for node classification. *In Proceedings of the ACM Web Conference 2022 (pp. 1028-1036)*.

Zhang, X., Fu, J., & Li, S. (2023). Contrastive Disentangled Learning on Graph for Node Classification. *arXiv preprint arXiv:2306.11344*.